ACS Catalysis

Review

pubs.acs.org/acscatalysis

Critical Literature Review of the Kinetics for the Oxidative Dehydrogenation of Propane over Well-Defined Supported Vanadium Oxide Catalysts

C. A. Carrero,*[,†,§,#] R. Schloegl,[‡,§] I. E. Wachs,[∥] and R. Schomaecker[†]

[†]Department of Chemistry, Technical University of Berlin, Straße des 17. Juni 124, D-10623 Berlin, Germany

[‡]Department of Inorganic Chemistry, Fritz Haber Institute of the Max Planck Society, Faradayweg 4-6, 14195 Berlin, Germany

[§]Department of Heterogeneous Reactions, Max Planck Institute for Chemical Energy Conversion, Stiftstraße 34−36, D-45470 Mülheim an der Ruhr, Germany

[∥]Operando Molecular Spectroscopy and Catalysis Laboratory, Department of Chemical Engineering, Lehigh University, 111 Research Drive, Bethlehem, Pennsylvania 18015, United States

Supporting Information

ABSTRACT: Producing propene by the oxidative dehydrogenation of propane (ODH) has become an attractive and feasible route for bridging the propene production-demand gap, either as a complementary route of the existing oil-based processes or as a new alternative from propane separated from natural gas. The industrial application of propane ODH has not succeeded so far due to low propene yields. Therefore, propane ODH has been extensively investigated in recent decades using different catalysts and reaction conditions. Although several important aspects have been discussed in previous reviews (e.g., supported vanadium oxide catalysts, bulk catalysts, productivity toward propene, etc.), other relevant aspects have not been addressed (e.g., support effects, loading effects, vanadia precursor or catalyst synthesis methods, surface impurities, structure−reactivity relationships, etc.). In this review, we endeavor to cover the majority of the publications with an emphasis on the following: (1) catalyst synthesis: to focus on the influence of synthesis methods on the final vanadium oxide surface species, (2) catalyst characterization: to identify the molecular structures of the supported vanadium oxide species as well as the oxide support surface physical and chemical characteristics, (3) kinetics: to understand how reaction rates depend on variables such as concentration of gas-phase reactants and temperature, (4) structure−activity relationship: to examine the influence of the concentration as well as molecular structures of the surface vanadium oxide species on the reaction kinetics, and (5) reaction mechanism: to use the structure−activity relationships as well as kinetic studies plus theoretical calculations to corroborate and/or propose reaction pathways that account for the overall ODP reaction mechanism.

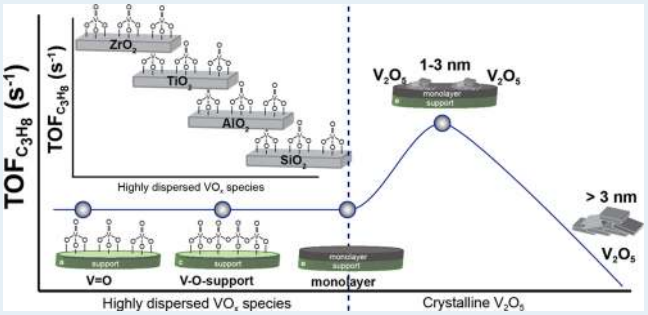

KEYWORDS: *catalysis, propane ODH, olefins, kinetics, monolayer, vanadia catalysts, kinetics*

INTRODUCTION

Propylene is a key commodity chemical for the petrochemical industry (Figure 1).[1] According to a 2012 study by HIS Chemical Market Associates, Inc. (CMAI),[2] on-purpose propylene technologies—including propane dehydrogenation (PDH), methathesis (MT), and methanol-to-olefins (MTO)—have a market share of up to 14% of the global propylene production (80 Mt/year in 2012),[3] and this share is expected to grow to over 20% in the near future.

The catalytic dehydrogenation of propane is the most direct and selective way to produce propylene. The reaction characteristics, however, pose inherent difficulties and certain technical constraints in developing commercial processes.[4] For example, thermal dehydrogenation of propane is strongly endothermic and requires operation at both high temperature and high paraffin partial pressure lower than 1 atm due to the increase in number of mols.[5,6]

The catalytic oxidative dehydrogenation (ODH) of propane is a promising alternative process to close the growing gap between the demand and production of propene. The advantage of the propane ODH reaction is that the reaction is (i) exothermic, (ii) thermodynamically unrestricted, (iii) operates at much lower temperatures, and (iv) minimizes coke deposition ensuring long-term stability of the catalyst. Due to undesirable consecutive and parallel combustion reactions, however, the propene yields are still not sufficient to satisfy

Received: March 15, 2014
Revised: August 8, 2014
Published: August 15, 2014

   dx.doi.org/10.1021/cs5003417 | ACS Catal. 2014, 4, 3357−3380

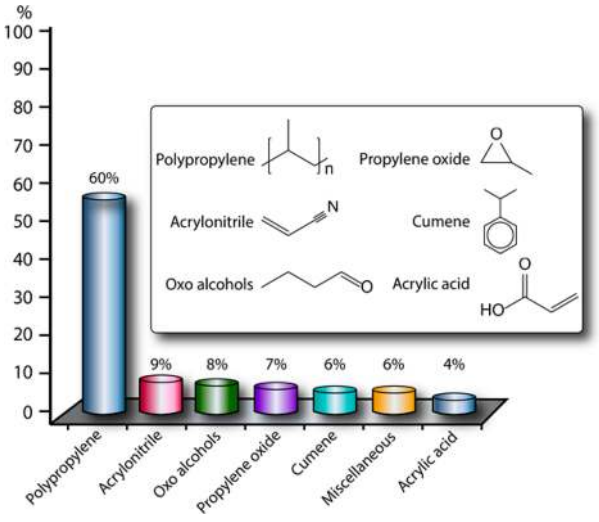

Figure 1. Main propylene derivates.[1]

economic feasibility. In other words, further increase of propene productivity based on propane ODH is a challenge that has yet to be overcome.

Despite the large number of literature reviews dealing with selective oxidation of light hydrocarbons,[7−12] both a comparative and critical overview of the propane ODH kinetics is still lacking. In 2006, Grabowski et al.[11] published a detailed review regarding the mechanism and kinetic models for ODH of alkanes. This first review has been exemplary and helpful in pointing out important kinetic details as well as the main problems of light alkanes' ODH. As the author expressed at that time, which to a large extent is still valid today, there are several fundamental questions facing the light alkanes' ODH, which are still awaiting solutions: (1) How do we stop the reaction at the stage of the desired compound (alkene) and eliminate its total oxidation, as the consecutive oxidation of alkene is the main source of carbon oxides and is responsible for low selectivity of the ODH process. (2) How are selectivity and activity of the catalyst related to the mechanism of this reaction? To answer these questions, many specific problems have to be solved. However, there are several aspects governing the ODH process that are generally accepted without being, however, unambiguously proven.

For example, the reaction occurs by a parallel-consecutive scheme in which carbon oxides are formed mainly by the consecutive overoxidation of the products (alkenes), whereas the direct combustion of the reactants (alkanes) plays a minor role. Moreover, it is well-known and accepted that the reaction proceeds by a redox mechanism previously described by Mars−van Krevelen.[13]

Recently, literature on both propane and ethane ODH catalysis was reviewed,[12] showing several different reaction conditions at which propane ODH can be carried out. The review focused on (1) the main features affecting the catalytic properties of systems based on supported vanadium oxide and molybdenum oxide, (2) characteristics of catalysts producing outstanding olefin yields, (3) the reaction network of partial and total oxidation, and (4) involvement of homogeneous gas phase reactions to the formation of olefins during the oxidative dehydrogenation of alkanes.

Although important propane ODH aspects were summarized and discussed in the above-mentioned reviews (e.g., supported vanadium and molybdenum oxide catalysts, bulk catalysts, conversion versus selectivity trajectories, productivity toward propene, contribution of homogeneous gas-phase reactions, etc.), other significant fundamental aspects have not been addressed (e.g., support effects, surface impurities, loading effects, vanadia precursor or catalyst synthesis methods, structure−reactivity relationships, in situ or operando studies, etc.). Clearly, there are still many important issues that need to be taken into account in summarizing the propane ODH literature.

Cavani et al.[12] gauged the propene productivity (expressed as $kg_{propene}/kg_{catalyst}$/hour) to compare the reported propane ODH results. Because some experimental aspects are missed, an accurate interpretation of the collected data becomes complicated. In order to obtain substantial insights, the comparison needs to be performed at similar reaction conditions, avoiding total oxygen conversion and homogeneous gas-phase reactions in order to allow appropriate assignments of the influence of either the catalyst or the reaction parameters.

Vanadium oxide is considered to be one of the most important and useful metals to be used as a catalyst due to its physical and chemical properties, and catalysis is the most dominant nonmetallurgical use of vanadia.[12] Vanadium oxide catalysts have been used in many industrial catalytic processes[4,15−17] and in numerous catalytic reactions on the lab scale that are awaiting further improvement so they can at least be applied on a large industrial scale.[18−21] In many cases, vanadia catalysts are doped with promoters to improve their activity or selectivity, while various supports are used to improve mechanical strength, thermal stability, longevity, and catalytic performance.

In the present ODH of propane literature, we endeavor to cover the majority of the large number of publications with an emphasis on the following: (1) *catalyst synthesis*, to focus on the influence of synthesis methods on the final vanadium oxide surface species; (2) *catalyst characterization*, to identify the molecular structures of the supported vanadium oxide species as well as the oxide support surface physical and chemical characteristics; (3) *kinetics*, to understand how reaction rates depend on variables such as concentration of gas-phase reactants and temperature. Moreover, kinetics provides a basis for manipulating process variables to increase the propane ODH rates and minimizing undesired parallel combustion rates; (4) *structure−activity relationship*, to examine the influence of the concentration as well as molecular structures of the surface vanadium oxide species on the reaction kinetics; and (5) reaction *mechanism*, to use the structure−activity relationships as well as kinetic studies in addition to theoretical calculations to corroborate and/or propose reaction pathways that account for the overall reaction mechanism.

The objective of the current review is to compile the propane ODH literature that includes both reliable catalyst characterization and kinetic data to allow establishing structure−activity/selectivity relationships for supported vanadium oxide catalysts. Reliable catalyst structural characterization translates into a clear verification of the presence of either highly dispersed surface vanadium oxide species or crystalline V_2O_5 nanoparticles in the investigated catalysts. The exact nature of the "surface oxide" vanadium species plays a critical role in terms of its local structure that is not addressed explicitly in many publications. Reliable kinetic data allow us to clearly consider the reaction rates, which are suitable for calculating other kinetic parameters. The frequently reported selectivity versus conversion plots are no substitute for the analysis of

dx.doi.org/10.1021/cs5003417 | ACS Catal. 2014, 4, 3357−3380

macrokinetic parameters even when they are useful to address the particular issue of selectivity control. The relevance of these plots is, however, limited when no information about the conversion level of oxygen is provided. In this way, the multitude of reports on ODH of propane limits itself to a small number in which all relevant data are available to allow comparison on the basis of the macrokinetic parameters. Compiling the literature results at similar reaction conditions requires some recalculations and assumptions that are suitable to extrapolate and normalize the reported ODH of propane rates. It guarantees a proper comparison in terms of catalyst activity and selectivity from which all derived information will be useful to identify correlations between catalyst properties and performance. Such calculations and assumptions are shown in the Supporting Information, S1.

Synthesis of Supported Vanadium Oxide Catalysts. The catalytic activity of vanadia is attributed to its reducible nature and its ability to easily change its oxidation state from V^{+3} up to V^{+5}.[22,23a] Whereas it is generally accepted that V^{5+} is the highly active initial state of the catalyst in a cycle of ODH, it is less clear what the lower reduced state may be. The stability of the V^{3+} oxidation state is not suitable for facile catalytic cycling and requires substantial electronic rearrangement, whereas the V^{+4} state, being less stable as isolated species, can easily convert back to V^{+5}. Theoretical arguments supporting the redox change by two formal oxidation states[23b] may depend critically on the assumptions of the theoretical model chosen. The answer to this question that may be different with different catalytic redox reactions (methanol oxidation vs propane ODH) is critical for determining the minimum size of an active site required to convert one propane molecule releasing two electrons.

Most vanadia-based catalysts consist of vanadia phases deposited on the surface of SiO_2, Al_2O_3, TiO_2, and ZrO_2 supports with fewer studies reporting on vanadia supported on CeO, NbO_5, MgO, and zeolites. The manner in which the vanadium oxide is deposited onto a support can have a significant influence on the properties of the active component in the final catalyst. Typically, the main method of dispersing vanadium oxide on support materials is the classic incipient wetness impregnation method in a solvent where the V-salt precursor is soluble. Both adsorption from solution (grafting) and ion exchange methods have also been used extensively. To a lesser extent, other catalyst synthesis methods have been used, such as vapor-fed flame synthesis,[24] flame spray pyrolysis,[25,26] sputter deposition,[27] and atomic layer deposition.[28] Chemical vapor deposition (CVD) uses volatile molecular metal precursors [i.e., $O{=}VCl_3$,[29,30] $O{=}V(OC_2H_5)_3$,[31] or $O{=}V(OiPr)_3$[32a]] to modify oxide support surfaces and provides a way to control the dispersion of the active sites.

The impregnation method is most often employed to synthesize vanadium oxide catalysts for propane ODH. It is performed by contacting the support with a certain volume of solution containing the dissolved vanadium oxide precursor. If the volume of the solution is either equal or less than the pore volume of the support, the technique is referred to as incipient wetness.[33] This particular synthesis route shows a broad variation of vanadium oxide surface species at loadings below monolayer coverage, depending on the synthesis conditions. Furthermore, it offers little control over surface species and their dispersion. This method may also lead to the formation of three-dimensional V_2O_5 nanoparticles, even at low vanadium oxide loadings.[22] A variety of recipes, based on the impregnation method using ammonium metavanadate as the precursor, have been reported. A mixture of water with oxalic acid, using methanol as a solvent instead of water, and varying the acidity of the solution have been also reported in order to improve the precursor solubility, which leads to better vanadium oxide dispersion on the support material.[34−36] On the other hand, impregnation of different supports, starting with soluble organic precursors such as solutions of either vanadyl acetylacetonate ($VO(acac)_2$) in toluene,[37−39] ($VO(iPrO)_3$, $VO(OC_2H_5)_3$, or $VO(OC_2H_7)_3$ in 2-propanol,[40,42] have shown that higher amounts of supported vanadium oxide can be dispersed onto the support material, leading to highly dispersed catalysts without V_2O_5 nanoparticles below the monolayer coverage. This is due to the higher solubility of the last-mentioned precursors in comparison to NH_4VO_3.

Adsorption from the solution or grafting methods, also known as the anchoring method, are based on attaching vanadia from the solution through reaction with the hydroxyl groups on the surface of the support, because the surfaces of the support materials are mainly composed of oxygen atoms and hydroxyl groups. Several grafting methods have been widely used to prepare supported catalysts.[43−45] The grafting method helps to achieve a high percentage of metal loading and also helps to disperse the active metal sites by appropriately tuning the preparation procedures. The ion exchange method permits the ionic vanadium oxide species present in an aqueous solution to be electrostatically attracted by charged sites of the support surface. It allows, for example, the controlled introduction of more vanadium oxide species into MCM41 by keeping its mesoporous structure, which is not always the case with the direct hydrothermal method.[46] A summary of the design strategies for the molecular-level synthesis of supported catalysts can be found elsewhere.[47]

The issue of synthesis from aqueous phase is severely complicated by the extreme nature of isolated V-species to form condensates into isopoly vanadates. Only at extreme pH values, at which surfaces of supports would dissolve, is it clear that V species are monomolecular. Because the ioselectric point of the support is not always considered when preparing the impregnation solution, it is not clear if adsorption by ion exchange or deposition−precipitation is the true synthesis reaction. The most critical step in controlling the nuclearity of the species is the drying procedure, as there the pH changes drastically. This step is usually poorly controlled and thus little is known about the condensation process of the initial V species. In summary, it is no surprise that a broad variety of V_xO_y species may result from a nominally "simple impregnation" process, and the assumption that the nuclearity of the V species is controlled by its abundance relative to the geometric surface area of the support is quite uncertain in the absence of evidence that opportunity was given to the system to disperse into isolated species bound to surface hydroxyls.

Another method, which has shown interesting results in terms of vanadium oxide dispersion, is the flame spray pyrolysis method (FSP).[48−51] It offers a relatively simple, rapid and scalable synthesis capable of producing high sample amounts (e.g. 1.1 kg/h of nanoparticles),[52] but traces of Cl surface impurities also result from employing the FSP method.[53]

It is important to emphasize that, besides the aforementioned methods employed to disperse vanadium oxide on different material supports, the calcination treatment used for the fixation of the vanadia is a crucial step of the catalyst preparation. At high calcination temperatures, mixed oxide

dx.doi.org/10.1021/cs5003417 | ACS Catal. 2014, 4, 3357−3380

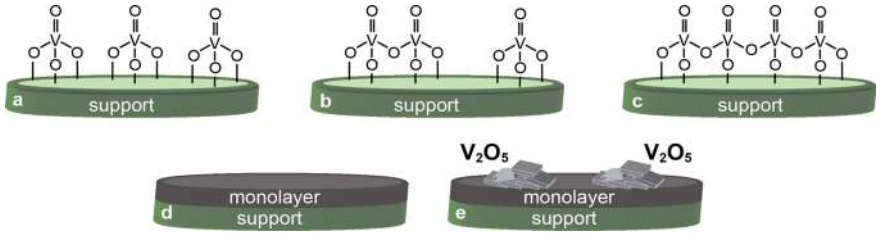

Figure 2. Structures of supported vanadium oxide catalysts formed at loadings below (a–c), reaching the monolayer (d), and above the monolayer coverage (e).

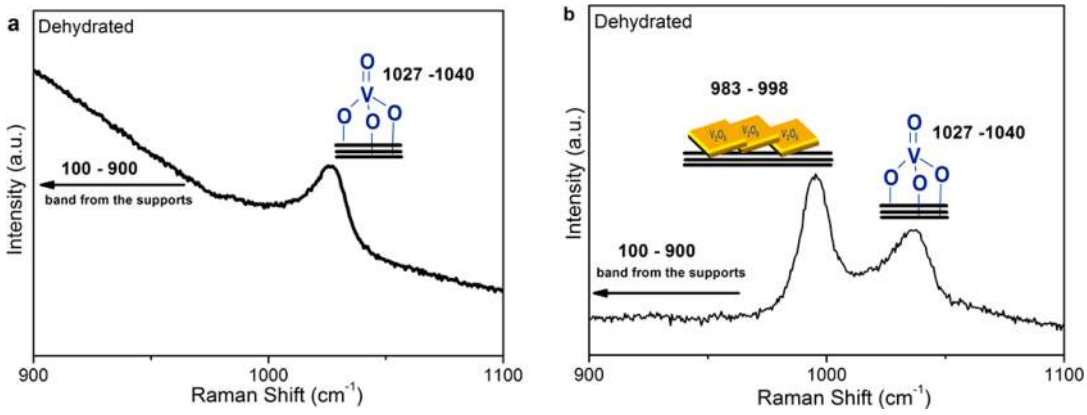

Figure 3. Typical in situ Raman spectra of dehydrated (a) highly dispersed surface VO_4 species and (b) surface VO_4 species and three-dimensional V_2O_5 NPs. The position of the Raman vibrations only slightly depends on the oxide support material and surface vanadia coverage as given in the literature.[71−75]

compounds or solid solutions can be formed with some oxide supports (e.g., $Zr(V_2O_7)_2$[54−56] and $AlVO_4$[57]). Also, it is important to note that the majority of the above-mentioned methods, except for the FSP method, are inherently limited in scalability. Most of them have been employed to prepare small catalyst amounts, generally used as model catalysts. Although they have shown reproducibility on laboratory scale, batch effects cannot be excluded completely. Scaling the catalyst production, which is added to its cost, is still a challenge to take into account before employment of a possible synthesis method. For example, a considerably high amount of catalyst (ca. 8 g) has been prepared by grafting alkoxide precursors on SBA-15.[58]

In summary, the relative concentrations of the surface vanadia species on oxide supports strongly depend on the specific oxide support, surface vanadium oxide density, catalyst synthesis method, preparation conditions, solvents, and temperature of calcination. New insights into the preparation of supported vanadium oxide catalysts are expected in the future. The molecular design of highly effective catalysts requires tuning concepts from solution chemistry, solid-state chemistry, and inorganic chemistry for preparing catalysts. This would require future investigations on the issue to have a more careful control of the synthesis conditions and a detailed description of the synthetic parameters, thereby allowing the assessment of the exact sequence of inorganic reactions leading to the active catalyst. Only then will it be possible to have a meaningful comparison of properties that is based upon comparing the same state of the same species .

Characterization of Vanadium Oxide Catalysts. Quantitative structure–activity/selectivity catalytic relationships can only be established once characterization of the catalysts provides fundamental information about the surface vanadium oxide species, especially under reaction conditions (for instance, the oxidation state of vanadia, its coordination environment, molecular structures of the different vanadia species, and number of catalytic active vanadia sites participating in the reaction). Multiple characterization techniques are usually required to obtain a complete understanding of supported vanadium oxide catalysts. Fundamental information about the molecular and electronic structures of supported vanadium oxide phase(s) in powdered catalysts are typically obtained by in situ FTIR, UV–vis, Raman, solid-state NMR, and electron paramagnetic resonance (EPR) spectroscopy.[59,60] Ultrahigh vacuum and theoretical experiments also provide relevant information about the different surface vanadia species formed on model oxide support.[61] Corresponding information about the surface chemical properties can be obtained with XPS and XAS[62,63] surface analysis. Operando spectroscopy studies that simultaneously combine spectroscopic observation of surface phenomena with catalytic performance have recently been introduced and have become the cutting edge approach in catalysis research to establish structure–activity relationships.[64] Recently, a quasi-in situ approach has been used for elucidating the species coexisting on the catalyst surfaces before, during, and after propane ODH reaction.[60b] The evolution of spectroscopic instrumentation for catalyst characterization since the 1950s can be found in ref 65, and the detailed fundamental aspects of each spectroscopic technique can be found elsewhere.[59,60a,66−69]

The different vanadia phases that can be present in supported vanadium oxide catalysts are illustrated in Figure 2. The distribution among the different vanadium oxide structures depends on the synthesis method, V-precursor, solvent, calcination temperature, vanadium oxide loading, oxide support, and so forth.

dx.doi.org/10.1021/cs5003417 | ACS Catal. 2014, 4, 3357–3380

Table 1. Reported Vanadia Surface Densities at Which the Experimentally Determined Monolayer Coverage Is Reached

support	BET surface area [m^2/g]	vanadia surface density [V_{atom}/nm^2] – (V_2O_5 wt %)	synthesis method (precursor–solvent)[a]	ref
SiO_2	~333	3.3 (15)	FSP (AMV–H_2O)	50
Al_2O_3	~222	9.3 (23.7)	IWI (V_{iso}–2-propanol)	83
TiO_2	~45	9.2 (5.9)	IWI (V_{iso}–2-propanol)	83
ZrO_2	~34	8.1 (4)	IWI (V_{iso}–2-propanol)	83
CeO_2	~36	9.2 (4.8)	IWI (V_{iso}–2-propanol)	83
Nb_2O_5	~57	7.6 (6.1)	IWI (V_{iso}–2-propanol)	83

[a]FSP = flame spray pyrolysis. AMV = ammonium methavanadate. IWI = incipient wetness impregnation. V_{iso} = vanadium isopropoxide.

At loadings below monolayer coverage (Figure 2a–c), isolated and oligomerized surface VO_4 species are present on the oxide support. The surface VO_4 species possess three different oxygen atoms: (i) oxygen atom forming a vanadyl group (V=O), (ii) oxygen atom bridging two vanadia atoms (V–O–V), and (iii) oxygen atom bridging a vanadia atom and oxide support cation (V–O–Support). Depending on the vanadia surface density as well as the support material, a vanadia monolayer coverage can be reached (Figure 2d).

Monolayer coverage represents completion of a 2D surface vanadium oxide overlayer on the oxide support, and the surface becomes saturated immediately before 3D V_2O_5 crystallites start to grow (Figure 2e). The concept of the oxide monolayer was first suggested by Russell and Stokes in 1946.[70] The preparation, characterization, and catalytic activity of vanadium oxide monolayer catalysts have been reviewed.[22] The different surface vanadia species are mostly identified by Raman spectroscopy (Figure 3)[71−75] and UV–vis spectroscopy.[76,77] The 3D V_2O_5 nanoparticles (NPs) can be detected with XRD (only for NPs > 4 nm),[78,79] and all V_2O_5 NPs can be detected with Raman spectroscopy.

Raman spectroscopy is an extremely powerful and versatile technique for characterizing supported metal oxide catalysts and, in particular, supported vanadium oxide catalysts, because it can provide fundamental information about the possible presence of multiple molecular structures of the active sites during propane ODH. Most of the employed support materials are not Raman-active or at least not in the region where vanadium oxide species exhibit Raman bands.

Different molecular densities were determined for monolayer surface coverage of vanadium oxide catalysts on different support material based on Raman spectroscopy (Table 1). With the exception of SiO_2, it is generally agreed that surface vanadia monolayer coverage corresponds to ~8–9 V atoms/nm^2. The lower maximum dispersion of vanadia on SiO_2 is related to the lower reactivity of the silica surface. Although V_2O_5 NPs are expected to be present at vanadium oxide loadings greater than monolayer coverage, V_2O_5 NPs can also be present below monolayer coverage when the precursor salt is not well-dispersed over the oxide support in the synthesis step or when a weak interaction exists between the vanadium oxide and the support (e.g., with SiO_2). Both cases lead to the formation of V_2O_5 particles, even at vanadia loading far below monolayer coverage.

A supported V_2O_5 catalyst containing only surface vanadia species gives rise to the Raman spectrum shown in Figure 3a. The surface VO_4 species gives rise to a Raman band at 1027–1040 cm^{-1}, corresponding to the vanadyl bond (V=O) vibration, and the crystalline V_2O_5 NPs exhibit a band at 983–998 cm^{-1}, corresponding to the short unperturbed isolated V=O bond. The nuclearity of the V_xO_y species and its unequivocal detection by RAMAN spectroscopy are of critical nature for controlling the catalyst selectivity. Three-dimensional V_2O_5, despite its apparent layer structure, is a material catalyzing exclusively total combustion of hydrocarbons through its surface sates arising from the n-type semiconducting nature[4] of the compound. This indicates that the electronic properties of V_xO_y in pure form cannot explain the catalytic selective oxidation behavior.

Surface impurities can also have a pronounced effect on the activity and selectivity of supported vanadia catalysts.[32a] Noninteracting surface impurities preferentially coordinate with the oxide support rather than the surface vanadia sites. Noninteracting surface impurities can only indirectly affect the molecular structure of the surface vanadia sites via lateral interactions. The addition of noninteracting surface WO_x and MoO_x sites to supported V_2O_5/Al_2O_3 catalysts increased the propene ODH activity by a factor of ~2 and did not affect the propene selectivity.[32b] It was proposed that these non-interacting additives promote the propane adsorption step by weakly interacting with propane in a precursor state that supplies propane to the surface VO_x sites. Interacting surface impurities preferentially interact with the surface vanadia sites rather than the oxide support to perturb the structure of the surface vanadia sites. For example, surface PO_x can react with surface VO_x to form crystalline $VOPO_4$ nanoparticles and surface alkali can complex with the surface vanadia sites to alter the local structure and suppress the redox activity.[32c,d] Such interacting additives usually have a negative effect on the activity and possibly also selectivity of the supported vanadia catalysts for oxidation reactions. Thus, it is also important to know if the oxide supports being used are clean of surface impurities (e.g., XPS or low energy ion scattering (LEIS)) and to make sure that no surface impurities have been introduced during the catalyst synthesis procedure. Unfortunately, very few studies report surface analysis information for supported vanadia catalysts and their presence can occasionally complicate comparison of kinetics from different catalysis laboratories.

In summary, combining the results from such spectroscopic studies with the corresponding reaction kinetic data can allow a molecular-level understanding of the catalyst's structure–activity/selectivity relationships. A significant new addition to this task was achieved by explaining the fine structure of the V L edge spectra by first-principles theory.[80] This assignment gives now access to the details of the ligand field around a V species that in principle can be determined in situ as well as ex situ. On the basis of the structural variability of a V_xO_y active site cluster that satisfies the condition of activating an oxygen molecule, it will be soon possible to predict the exact local geometry of a V_xO_y site. Great care with the structural assumptions (e.g., for metal oxygen bond angles) was shown recently for the related case of a Mo oxide monolayer catalyst.[81]

The section shows that there is now a clear and proven methodology to establish the nature of a supported V_xO_y

dx.doi.org/10.1021/cs5003417 | ACS Catal. 2014, 4, 3357–3380

species at least in the limit of a monolayer system and in discriminating two-dimensional from three-dimensional systems and their possible mixtures. What is less clear is the nature of dynamical aspects of the catalyst. Under methanol oxidation conditions, it is possible that for weakly anchored species the formation of methoxy can mobilize the V_xO_y and lead to redispersion or agglomeration of the active phase. But also on strongly binding substrates, such as titania, it is expected and was verified that active vanadia species undergo structural dynamical changes upon redox changes. Because these changes are associated with the catalytic function and with the breaking and forming of V═O bonds (and also because water and OH are present in stoichiometric amounts and the reaction temperature is high enough to allow self-diffusion of oxygen ions), it is not clear at all if the ex situ determined structures of V_xO_y are also present and relevant under the reaction conditions or if these known structures are merely resting states or precursors to less-well-known active states. Experimental results point in this direction but require additional confirmation and general validation.[82,84] This caveat may be taken into consideration when we discuss later the modes of operation of such catalysts, assuming that we have a clear view on the structure and composition of active sites.

1. KINETICS OF OXIDATIVE DEHYDROGENATION OF PROPANE OVER VANADIUM OXIDE CATALYSTS

As mentioned before, enhancing the selectivity as well as the productivity toward propene through partial oxidation of propane under oxygen atmosphere has been a great challenge during the last two decades. Many researchers have been focusing either on developing new catalysts or improving the available ones with the purpose of reaching industrially applicable propene yields.[12] Despite these kinetic studies playing an important role in sorting out this challenge, only a limited number of publications that describe a detailed propane ODH kinetic study are found in the vast propane ODH literature. Moreover, the common denominator of the majority of publications is the missing connection between reactivity and catalytic active site structure. Most publications focus on the catalytic reactivity and propene yield (mostly showing the propene selectivity/yield vs propane conversion plots) without deepening either the kinetic details (e.g., reduction−oxidation constants, propane/propene oxidation activation energies, reaction orders, etc.) or the reaction mechanism.

Different kinetic models[85−89] have been used for the kinetic description of the oxidative dehydrogenation of light alkanes as listed in Table 2: (1) Mars−van Krevelen model (MvK), (2) Eley−Rideal model, (3) Langmuir−Hinshelwood model, and (4) Power Law model. The MvK model is the most suitable for describing the oxidative dehydrogenation of propane over different supported vanadium oxide catalysts,[56,90−92] although the MvK model has also been considered as inconsistent and incorrect for general reduction−oxidation reactions on solid catalysts.[93]

Grabowsky et al.[11] published a review in 2006 focusing on the kinetics of oxidative dehydrogenation of light alkanes with propane ODH kinetics by supported vanadium oxide catalysts as one of the crucial discussion points. By taking into account just the reaction kinetics and kinetics modeling, the authors pointed out the initial propane ODH kinetic works that established the first-needed procedures to kinetically explain how the production of propene from the oxidative dehydrogenation of propane takes place. This review not only summarized relevant information about the variety of kinetic models employed for propane ODH but also pointed out discrepancies between the different kinetic models using mostly residuals of fitting procedures. Moreover, it summarized the assumptions on which employed kinetic models were based.

Table 2. Different Rate Laws Reported for Propane ODH over Different Vanadium Oxide Catalysts[a]

mechanism	general kinetic equation	examples
MvK (lattice oxygen)	$r = \frac{k_{ox} k_{red} p_{O_2}^{\ n} p_P}{k_{ox} p_{O_2}^{\ n} + k_{red} p_P}$	56, 90-92
Eley−Rideal (reaction between adsorbed O_2 and gaseous or weakly adsorbed R)	$r = \frac{k_{O_2}^n p_{O_2}^n p_P}{1 + k_{O_2}^{\ n} p_{O_2}^n}$	94, 96
Langmuir−Hinshelwood (uniform surface with one type of site)	$r = \frac{k_{O_2}^n k_P p_{O_2}^n p_P}{(1 + k_{O_2}^n p_{O_2}^n + k_P p_P)^2}$	97
Power Law	$r = k p_{O_2}^n p_P^m$	98-99

[a] r is the reaction rate; k, the reaction rate constant; k_{ox}, k_{red}, the rate constant of oxidation or reduction; n = 1 or 0.5 for O_2 molecular or dissociative adsorption; P, propane; K_{O_2}, K_P, the adsorption coefficient of O_x or P; a, the stoichiometric coefficient.

As an example, Creaser et al.[100] proposed a Langmuir−Hinshelwood model assuming that either all the reactants adsorbed on the same site or that oxygen adsorbs at separate sites and propane reacts directly with oxygen on the catalyst's surface. It was also assumed that equilibrium is established between the adsorbed and gas-phase propene when carbon oxides are produced in a consecutive reaction. In the same paper, two types of MvK models were also considered. The first MvK model was based on the assumption that the reaction rate is proportional to both the pressure of propane and the fraction of free sites. In the second MvK model, the reaction rate was assumed to depend on the degree of the oxidation of the catalyst. All the models fit in the experimental data with similar fitting errors, and MvK type models fit the data satisfactorily without any large correlation between the parameters; however, in the opinion of the authors, the MvK mechanism was most suitable for the description of the experimental data.[11]

Grabowsky et al.[11] also summarized and presented relevant kinetic data as well as the rate equations employed in the data analysis. The author clarified every assumption for each reviewed publication which highlights this review. As the authors pointed out, this review was to survey the main facts and concepts on the kinetics of oxidative dehydrogenation of light alkanes, taking into account the main catalysts employed until that date. Important to notice is the fact that the author quoted less than 18 papers for propane ODH during the period of 1994 to 2006. Studying the influence of the type of support, promoters, acid−base properties, and type of oxygen on the performance of oxidative partial reactions was also discussed. It was remarkably concluded that ODH of light alkanes is almost always described by the parallel-consecutive reaction network, in which both the selective reaction (formation of alkene) and consequent oxidation to carbon oxides and parallel direct formation of carbon oxides have taken place. Kinetic investigation evidenced that COx is formed mainly by consecutive oxidation of alkene and to a lesser extent on parallel route by direct oxidation of alkane. The author also remarked that the MvK mechanism is most frequently proposed for describing of the kinetics of ODH of light

dx.doi.org/10.1021/cs5003417 | ACS Catal. 2014, 4, 3357−3380

alkanes. Other mechanisms are used rather scarcely and mainly for the kinetic description of paths in ODH of alkanes in which COx is formed.

With regard to the lattice oxygen participating in the ODH reaction, it is widely accepted that combustion reaction occurs with the participation of adsorbed oxygen. Some authors, however, consider that two forms of oxygen (electrophyllic-adsorbed oxygen, nucleophyllic-lattice oxygen) are present on the surface of the catalyst. Lattice oxygen is usually considered to be responsible only for selective reactions, but some authors link it to both selective ODH and total oxidation. In the case of vanadia-containing catalysts, only one type of oxygen is responsible for ODH and total combustion reactions. For example, in the case of ODH of propane, out of nine papers that focus on the modeling of its kinetics, only three assume the existence of two forms of oxygen on the catalyst surface.[101−103]

A conceptual shortfall of a "Mars−van Krevelen mechanism" in its original meaning is that in a (sub) monolayer catalyst it is hard to identify a "lattice" oxygen species as such a catalyst has only surface atoms. Unclear implications are then that oxygen species from the support may come into play and the "support" becomes a cocatalyst or that the original definition of lattice is relaxed to "surface lattice",[104]which is then only a semantic difference to a chemisorbed atomic oxygen species. It would be most useful to avoid the term Mars−van Krevelen and state specifically to what structural property (oxygen abundance, oxidation state, binding energy of oxygen, oxygen species) the kinetic model is referring, because the mathematical form of a macrokinetic equation makes no explicit statement about an atomic nature of relevant species. The often referenced microscopic argument of isotope exchange kinetics is a critical argument, because the chemical potential that controls this exchange kinetics is hardly taken into account, and the fact that an oxide can slowly exchange oxygen species does not imply that its catalytic function relies on this property.[105]

The shortcoming of this excellent kinetic review[11] is that the details about the catalyst properties (synthesis and characterization) were not emphasized, mostly due to the fact that the original studies did not present this information. Although the apparent activation energy was used to study the support and promoter effect, several parameters are different from each other, diminishing the accuracy of the comparison.

The present review attempts to rigorously compare experimental kinetic results found in literature for vanadium oxide supported on TiO_2, ZrO_2, Al_2O_3, and SiO_2. The selected parameters for the comparative study are the (1) reaction temperature (°C), (2) apparent activation energy for oxidative propane dehydrogenation (kJ/mol), (3) propane consumption turnover frequency (s^{-1}), (4) catalyst surface area (m^2/g), (5) V_2O_5 loading (wt %), (6) surface vanadia density (V_{atoms}/nm^2), and (7) catalyst synthesis method. These parameters are further described in the Supporting Information, S2.

From the vast available literature for propane ODH by supported vanadium oxide catalyst, only a limited number of papers satisfied the criteria given above. Attempting to include as many carefully performed works as possible, and using data originally reported in these papers, some recalculations, assumptions, and considerations had to be made in order to be able to perform side-by-side comparisons that required the following experimental conditions.

Experimental Requirements.

(1) Carrying out the experiments at temperatures distant enough from temperatures where homogeneous gas-phase reactions start to occur, perturbing both the overall reaction rate and the desired product selectivity. At such elevated temperatures (>550 °C), it is difficult to distinguish and separate the contribution of homogeneous gas-phase reactions from the catalytic reactions taking place at the same time.

(2) Author: Please verify that the changes made to improve the English still retain your original meaning.Using V_2O_5 loadings only up to the monolayer coverage, because highly dispersed vanadium oxide is an important prerequisite for achieving high propylene selectivity. Studying data of highly dispersed catalysts with loadings below vanadium oxide monolayer coverage allows investigating the influence of different vanadium oxide species in propane ODH. Below monolayer coverage, all the vanadia sites are exposed to the reactive environment and permits for quantitative determination of the catalytic turnover frequency (number of propane molecules converted per V atom per second) that will allow comparison of different catalyst studies. This method of quantification assumes that only one species of V_xO_y exists under reaction conditions and that there is no resting state or dynamical deactivation of the active form. The presence of three-dimensional aggregates requiring additional correction factors that are hard to justify would further complicate estimation of even an upper limit of active sites for propane oxidation. For the purposes of a comparative discussion of the performance of monolayer catalysts, we use the concept of turnover frequencies always keeping in mind its limitations pointed out here.

(3) Performing kinetic experiments at low propane conversions, preferably below 10%, in order to guarantee differential conditions. Moreover, higher propane conversions require severe reaction conditions which also accelerate the parallel propane combustion perturbing the overall reaction rates and as a consequence, the propane dehydrogenation activation energy. Because oxygen, rather than propane, is the limiting reactant, low propane conversions are desired; otherwise, high and even total oxygen conversion is expected. Low propane conversion is achieved by lowering the residence time.

(4) Discarding kinetic data obtained under transient conditions, thereby collecting only data obtained at steady-state conditions.

(5) Excluding data obtained over binary-promoted or doped catalysts, because the active center involved in the reaction would not be clearly identified. For the same reason, multicomponent catalysts (e.g., V/Ti/Si or M1 type catalysts) are also excluded from the comparison.

(6) Excluding both internal and external mass transport limitations that could perturb the overall propane ODH reaction rate.

(7) Minimizing heat transfer effects which are intimately linked to mass transport limitation. The accumulation of both reactants and products in any location on the catalyst bed would facilitate the formation of hot spots, leading to undesired total combustion reactions.

(8) Avoiding total oxygen conversion in order to guarantee catalyst stability against coke formation and utilization of an ill-defined fraction of the catalyst bed.

dx.doi.org/10.1021/cs5003417 | ACS Catal. 2014, 4, 3357−3380

Table 3. Summary of Propane ODH Kinetics for Supported V_2O_5/TiO_2 Catalysts and Catalyst Properties from Selected Publications

$E_{a\,1}$ [kJ/mol]	$TOF_{propane}$ [$\times 10^{-3}$ s^{-1}]	temp [°C]	BET [m^2/g]	V_2O_5 [% wt]	V [atom/nm^2]	synthesis method (precursor−solvent)[a]	ref
44−76	2.2−12.9 (400 °C) 6−74 (500 °C)	300−500	106−111	1.0−5.8	0.6−3.6	IWI (AMV−H_2O)	111
65−73	26−28 (380 °C) 36−42 (400 °C) 163−226 (500 °C)	340−400	43−49	1−3	1.4−4.6	IWI (AMV−H_2O)	112
43−51	1−7 (300 °C) 4.9−26.4 (400 °C) 160−50 (500 °C)	300−550	29.1−46.8	1.3−9.7	1.8−22	IWI (AMV−H_2O)	113
54		400	40−41	783−765	3.2−6.6	IWI (AMV−H_2O)	92
	18.5 (400 °C) 126.1 (500 °C)	500	41	5	8.1	IWI (AMV−H_2O)	114
	20.4 (400 °C) 101 (500 °C)	450−500	35.3	3.87	7.1	IWI (AMV−H_2O)	115
70	15.7 (400 °C) 79.2 (500 °C)	250−600	43	5	7.7	IWI (AMV−H_2O)	116
56	58 (400 °C) 212 (500 °C)	250−350	66	1.6	1.5	grafting (VAc.−toluene)	37
	18.6 (400 °C) 126.4 (500 °C)	500	41	5	8.1	IWI (AMV−H_2O)	117
	0.5−2.4 (333 °C) 1.5−12.4 (400 °C) 5.5−84.2 (500 °C)	333	58−73.5	0.7−5	0.63−5.7	IWI (AMV−H_2O)	118

[a]IWI= incipient wetness impregnation. AMV = ammonium methavanadate. OA= oxalic acid. VAc.= vanadium acetyl acetate.

(9) Guaranteeing catalyst stability against sintering of the active vanadium oxide species or the collapse of the support oxide structure affecting the propane ODH kinetics.

(10) Finally, carbon balance is a very important aspect to consider, which ensures that the kinetic data is calculated properly. Mostly at high propane conversion levels, carbon balance is strictly necessary to ensure accuracy in the obtained kinetic data.

In order to provide accurate kinetic data, all the aforementioned aspects should be taken into account. Peculiarly, the last five aspects (from 6 to 10) are still not considered in many published studies. Unfortunately, some publications show substantial deficits in some of these aspects.[106−110] Although none of the reviewed studies has studied how all these aspects influence the reaction rate, the comparative study made in the present review is based on results published considering some of the mentioned experimental requirements. In this review, mainly experimental data from differential reactors are compared because most authors used such reaction conditions. Carefully operated integral reactors and parameter evaluation by numerical fitting of kinetic models to the experimental data would also provide information about the reaction network. In addition, some assumptions and recalculations were considered, which are explained in the Supporting Information. The propane ODH literature also contains many additional publications, but many of them are not considered here because they focus on nonkinetic aspects or do not fulfill the above critical selection criteria for the experimental conditions.

Taking into account the selected conditions to compare the data as well as considering the experimental requirements mentioned above, we carefully collected kinetic data from vanadium oxide catalysts supported on TiO_2, ZrO_2, Al_2O_3, and SiO_2 that are described and discussed in the sections below.

Supported V_2O_5/TiO_2 Catalysts. The supported V_2O_5/TiO_2 catalysts reported in the literature for propane ODH and their synthesis methods and kinetics are listed in Table 3. The majority of the supported V_2O_5/TiO_2 catalysts were prepared by incipient wetness impregnation with aqueous NH_4VO_3 as the precursor. Many of the studies also added oxalic acid to the aqueous solution to enhance the poor solubility of AMV. Only one publication reported propane ODH kinetic data for supported V_2O_5/TiO_2 catalysts prepared by the grafting method using vanadyl acetylacetonate as precursor.[35] The reported activation energy values for propane ODH by the ed V_2O_5/TiO_2 catalysts are ~60 ± 12 kJ/mol. Regarding all data, the standard deviation is ±12 kJ/mol, but within one series of catalyst, the standard deviation is about ±5% as a function of surface vanadia coverage, synthesis method, and the laboratory performing the research, as shown in Figure 4. The kinetics at and/or above monolayer coverage was omitted because crystalline V_2O_5 NPs may be present in these studies and therefore may complicate determination of the apparent propane ODH activation energy. It is because V_2O_5 NPs catalyze the overall propane ODH reaction with substantially different apparent activation energies. A resolution of the kinetic parameters of this two different vanadia species is impossible.

The reported TOFs for propane ODH by supported V_2O_5/TiO_2 are rather similar at high surface vanadia coverage but quite different at low surface vanadia coverage, as presented in Figure 5. One set of researchers, Deo et al.[112] and Christodoulakis et al.,[113] reported almost constant TOFs as a function of surface vanadia loading, whereas a second set of researchers, Viparelli et al.[111] and Khodakov et al.,[118] reported that the TOFs increase with surface vanadia loading (Figure 5). A closer examination of the source of the TiO_2 support indicates that the group employing Degussa P-25 titania exhibits TOFs that are higher and constant with surface vanadia

dx.doi.org/10.1021/cs5003417 | ACS Catal. 2014, 4, 3357−3380

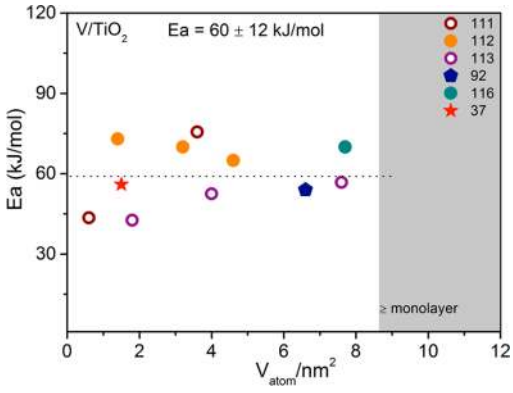

Figure 4. Apparent propane ODH activation energies as a function of vanadia loading on the TiO_2 support. The gray region indicates that the experimental monolayer surface vanadia coverage has been exceeded. The numbers indicate the cited references and the open symbols represent recalculated values that are explained in the Supporting Information.

coverage. It is well-known that Degussa P-25 is one of the cleanest titania supports and is the reference titania for photocatalytic studies.[121−124] The very similar TOFs for supported V_2O_5/TiO_2 catalysts from multiple catalysis research laboratories, when using the same TiO_2 support, is encouraging and demonstrates reproducibility between different catalysis laboratories.

The much lower TOFs at low surface vanadia coverage on TiO_2 reported by Viparelli et al.[111] and Khodakov et al.[118] requires closer examination of the TiO_2 supports used by these research laboratories. Both Viparelli et al.[111] and Khodakov et al.[118] employed high surface area TiO_2 supports from BASF and Süd-Chemie-AG, respectively, that extensively sintered when impregnated with vanadia and calcined at elevated temperatures. During such extensive sintering of an oxide support, the catalytic active vanadia phase may become incorporated by the titania support and, thus, not be able to participate in the catalytic oxidation reaction.[125]

Furthermore, the fraction of encapsulation may decrease with vanadia loading and, thus, may be responsible for the apparent increase in the TOF of propane ODH with vanadia loading. In contrast, the BET surface area of the P-25 titania support is relatively stable with vanadium oxide impregnation and calcination. Although the P-25 titania support is quite clean of surface impurities, surface chemical analysis for the BASF and Tioxide titania supports were not provided and, thus, the presence of surface impurities could not be ruled out. Furthermore, the increasing concentrations of V_2O_5 NPs with surface vanadia coverage in the Viparelli et al.[111] and Kodakov et al.[118] studies has also been demonstrated to give an apparent increase in TOF with coverage due to the anomalously high activity of the small V_2O_5 NPs that has recently been demonstrated by Carrero et al.[119] Consequently, TOFs of propane ODH with the supported V_2O_5/TiO_2 catalysts employing the P-25 titania support and not possessing V_2O_5 NPs provide the most reliable kinetics and demonstrate that TOFs of propane ODH are independent of the surface vanadia coverage (i.e., surface VO_4 monomer possess the same TOF as the surface VO_4 polymer). Alternatively, one can deduce from Figure 5 that two families of VO_x systems exist. One of them always contains the same type of active species, independent of the nominal loading, that does not scale with the nominal loading, as does its activity. The other family contains different amounts of active sites that scale in their abundance with the nominal loading. This may be deduced from the increasing TOF with the loading. In the limit of a monolayer loading, the two families converge in their properties as then the same amount of the same type of sites prevails. The kinetic parameters of these limiting catalysts should then be a reliable data set for further discussion.

Supported V_2O_5/ZrO_2 Catalysts. In comparison to supported V_2O_5/TiO_2 catalysts, an equal number of reliable propane ODH publications was encountered on supported V_2O_5/ZrO_2 catalysts. The reliable kinetic data as well as V_2O_5/ZrO_2 catalysts properties are listed in Table 4.

The majority of the published kinetic data is based on supported V_2O_5/ZrO_2 catalysts prepared by the IWI method with aqueous AMV as the precursor. In many of the syntheses, oxalic acid is also added to the aqueous solution because of the very low aqueous solubility of AMV. Two publications reported propane ODH kinetic data for supported V_2O_5/ZrO_2 catalysts prepared by incipient wetness impregnation of ZrO_2 using vanadium isopropoxide (VTiP) and 2-propanol as precursor and solvent, respectively.[40,42] Only one study reported propane ODH kinetic data for supported V_2O_5/ZrO_2 catalysts prepared by the grafting method using vanadyl acetylacetonate (Vac.) as the precursor.[37]

The apparent propane ODH activation energies over supported V/ZrO_2 catalysts as a function of vanadium oxide loading are plotted in Figure 6. The reported apparent propane

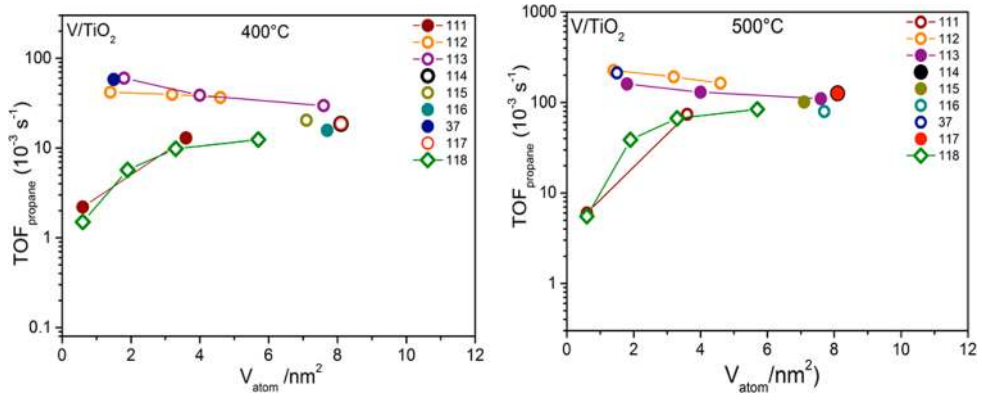

Figure 5. Propane consumption TOF rates as a function of surface vanadia coverage over supported V_2O_5/TiO_2 catalysts at (a) 400 and (b) 500 °C. The numbers indicate the cited references. Open symbols represent extrapolated values that are explained in the Supporting Information.

dx.doi.org/10.1021/cs5003417 | ACS Catal. 2014, 4, 3357−3380

Table 4. Summary of Propane ODH Kinetics for Supported V_2O_5/ZrO_2 Catalysts and Catalyst Properties from Selected Publications

$E_{a\,1}$ [kJ/mol]	$TOF_{propane}$ [$\times 10^{-3}$ s^{-1}]	temp [°C]	BET [m^2/g]	V_2O_5 [% wt]	V [atom/nm^2]	synthesis method (precursor−solvent)[a]	ref
94−112		340−500	82−36	5.6−15	4.5−9	IWI (AMV−H_2O)	126
	1.2−2.4 (333 °C) 11.2−9.0 (400 °C) 67.9−95 (500 °C)	333	180−340	2−30	0.4−5.5	IWI (AMV−H_2O)	56
	9.4−6.9 (350 °C) 28.4−67.3 (400 °C) 173−711 (500 °C)	300−350		0.4−4.0	0.8−8.1	IWI (VtiP−2-propanol	42
99	28.3 (430 °C) 13.3 (400 °C) 131 (500 °C)	430	170	10	3.9	IWI (AMV−H_2O)	127
51.1−81.1	0.1−1.5 (300 °C) 1.3−7.4 (400 °C) 10−60 (500 °C)	300−500	73.4−29.7	1.5−10.0	1.3−5.5	IWI (AMV−H_2O)	113
	6 (400 °C) 26 (500)	450−500	70.7	3.96	3.5	IWI (AMV−H_2O)	115
	18−80 (430 °C) 9.9−36.8 (400 °C) 60.2−388 (500 °C)	430	144−160	2−15	0.9−6.2	IWI (AMV−H_2O)	128
78	56 (400 °C) 340 (500 °C)	400	108	1.6	1.0	grafting (VAc.−toluene)	37
	1.5−2.6 (333 °C) 7−29.2 (400 °C) 42.5−309 (500 °C)	333	144−160	2−15	0.9−6.2	IWI (AMV−H_2O)	118
	9.8−10.2 (350 °C) 42.3−44 (400 °C) 447−465 (500 °C)	350		1−4	2.0−8.1	IWI (VTiP−2-propanol)	40

[a]IWI = incipient wetness impregnation. AMV = ammonium methavanadate. OA= oxalic acid. VAc. = vanadium acetyl acetate. VTiP = vanadium triisopropoxide.

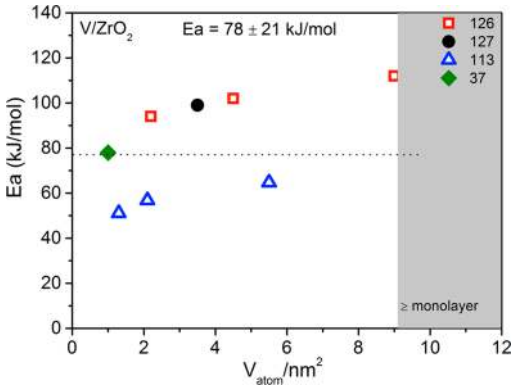

Figure 6. Apparent propane ODH activation energies as a function of surface vanadia loading on the ZrO_2 support. The gray region indicates that the experimental monolayer surface vanadia coverage has been exceeded. The numbers indicate the cited references. Open symbols represent recalculated values that are explained in the Supporting Information.

ODH activation energy over supported V_2O_5/ZrO_2 catalysts is ~78 ± 21 kJ/mol and slightly increases as a function of surface vanadia coverage and synthesis method. As can be seen by the limited data points in Figure 6, not many studies have been performed to determine the activation energy for propane ODH over supported V_2O_5/ZrO_2 catalysts.

The reported propane consumption TOFs over supported V_2O_5/ZrO_2 catalysts are rather different both in magnitude as well as in trend as a function of surface vanadia coverage as presented in Figure 7. Some researchers—Tian et al.,[40] Gao et al.,[42] Khodakov et al.,[56] and Christodoulakis et al.[113]—report almost constant TOF values as a function of surface vanadia loading, whereas Khodakov et al.[118] and Chen et al.[128] report increasing TOF values as a function of surface vanadia loading. In comparison to the other studies included in Figure 7, Khodakov et al.[56,118] and Chen et al.[128] are the only ones using zirconium oxyhydroxide ($ZrO(OH)_2$) as the support, which is prepared by precipitation from a zirconyl chloride solution. Due to morphological changes and sintering during calcination and reaction, a substantial fraction of the vanadia may be incorporated in the support material and excluded from the reaction. Nonetheless, Khodakov et al.[56] reported nearly constant propane consumption TOFs over catalysts similarly prepared, contradicting the rising TOFs obtained a few years later by the same researchers. This inconsistency invokes a detailed characterization of the support in order to figure out a possible interaction of unexpected species—"impurities"—and characterization of the supported vanadium oxide phase to determine if V_2O_5 and ZrV_2O_7 NPs are also present. The general shape of the plots in Figures 6 and 7 imply again that there may be families of catalysts with different structural properties likely related to the nuclearity or dispersion of the active species. In contrast to the TiO_2 support the data on the ZrO2 support do not allow a common likely data set for a comparative kinetic discussion as no convergence in trends can be observed. We note that some data sets in Figures 6 and 7 would agree well with the limiting data on titania and hence support the possibility that V_xO_y active sites perform the same reaction under the same conditions with the same kinetics independent of the support.

dx.doi.org/10.1021/cs5003417 | ACS Catal. 2014, 4, 3357−3380

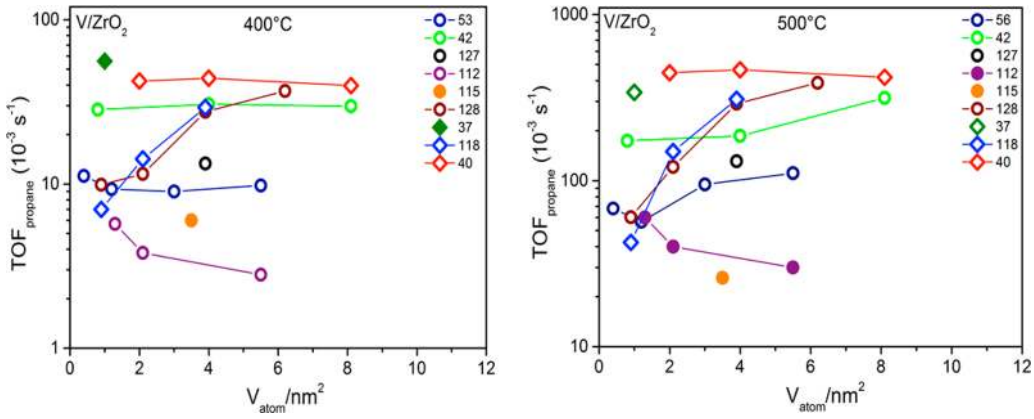

Figure 7. Propane consumption TOF rates as a function of vanadia coverage over V_2O_5/ZrO_2 catalysts at (a) 400 and (b) 500 °C. The numbers indicate the cited reference. Open symbols represent extrapolated values that are explained in the Supporting Information.

Supported V_2O_5/Al_2O_3 Catalysts. The supported V_2O_5/Al_2O_3 catalysts have been extensively studied, as can be seen in Table 5. As in the case for the support materials discussed previously, the majority of V_2O_5/Al_2O_3 catalysts are prepared by the IWI method using AMV as precursor. In many of the syntheses, oxalic acid was added to the aqueous solution to improve the AMV solubility. Few publications reported propane ODH kinetic data for V_2O_5/Al_2O_3 catalysts prepared by a grafting method using vanadyl acetylacetonate (Vac) as precursor.[37,38,129,130] Only a couple of studies were carried out for catalysts prepared by IWI method using vanadyl triisopropoxide and 2-propanol as precursor and solvent, respectively.[40,41]

Recently, highly dispersed V_2O_5/Al_2O_3 catalysts were prepared by the same method.[119,120] Dissolving V_2O_5 powder in oxalic acid followed by mixing the resulting solution with the Al_2O_3 support also appears to be an alternative method for preparing highly dispersed V_2O_5/Al_2O_3 catalysts.[131]

Compared to the previously discussed supports (TiO_2 and ZrO_2), several kinetic studies provide propane ODH activation energies. The reported apparent propane ODH activation energy over V_2O_5/Al_2O_3 catalysts is ~98 ± 12 kJ/mol and does not vary at all as a function of surface vanadia coverage, oxide support, synthesis method, and the laboratory performing the research (Figure 8).

Rao et al.[135] prepared supported V_2O_5/Al_2O_3 catalysts with vanadia surface densities close to monolayer coverage (~9 V_{atom}/nm^2) by the incipient wetness impregnation method using an aqueous solution of AMV avoiding the formation of V_2O_5 nanoparticles as corroborated by Raman spectroscopy. The obtained apparent propane ODH activation energy for such a catalyst was ~92 kJ/mol (Figure 8).[135] In contrast, V_2O_5 NPs were already present above ~3.6 V_{atom}/nm^2 with the same synthesis method reported by Argyle.[132] The catalysts containing V_2O_5 nanoparticles showed apparent propane ODH activation energies of ~120 kJ/mol, indicating that V_2O_5 NPs influence the propane ODH activation energy.[132]

Figure 9 describes the tendency of propane consumption rate as a function of vanadia surface density, and the reported TOFs can vary by more than 1 order of magnitude. In some cases, the TOFs remain almost constant from low to high vanadia surface densities,[38,40,131,135] whereas increasing TOFs as a function of vanadia loading are also reported in some studies.[41,118,128] Schwarz et al.[129] reported constant TOFs up to approximately 4.5 V_{atom}/nm^2. Above this surface vanadia coverage, the reactivity drastically dropped, but the absence of in situ characterization does not allow determination of the origin of this unusual behavior.

On the other hand, rising TOFs as a function of vanadia loading has been obtained from different authors but only from the same group.[41,118,128] In 1999, Khodakov et al.[118] published TOF values increasing as a function of vanadia loading over catalysts prepared by incipient wetness impregnation of Al_2O_3 with aqueous AMV solutions. A few years later, Chen et al.[128] once again reported increasing TOFs with vanadia loading over similarly prepared catalysts, perhaps even using the same catalyst batch. Comparing both studies, the only difference is the reaction temperature, which was 333 and 430 °C, respectively. Although the obtained TOF trend as a function of surface vanadia coverage was the same, considerable order of magnitude differences were reported that cannot be attributed to only the extrapolation from lower to higher temperatures. Moreover, subsequently, Yang et al.[41] reported the same trend of increasing propane consumption TOF as a function of surface vanadia loading over catalysts prepared by incipient wetness impregnation of Al_2O_3 but employing vanadium triisopropoxide in 2-propoanol solutions. Peculiarly, the data reported in the three above-mentioned studies are not consistent with each other and are the only studies reporting increasing TOFs as a function of surface vanadia loading. Surface characterization of these supports for surface impurities might have shed more light on the origin of these inconsistent kinetic results.

Tian et al.[40] prepared supported V_2O_5/Al_2AO_3 catalysts using the same procedure, but the TOF values were found to be constant as a function of surface vanadia coverage in contrast to that previously reported by Yang et al.[41] Both kinetic studies were carried out at similar reaction temperatures, indicating that the extrapolation should not dramatically influence the differences between both studies. What is different when comparing both studies, in terms of experimental conditions, is the fact that the C_3H_8 to O_2 ratio was different. Yang et al.[41] used a ratio of 8, whereas Tian et al.[40] used a ratio of 3. This indicates that the catalysts were more reduced at the high ratio C_3H_8/O_2 = 8 than C_3H_8/O_2 = 3. Although such different reaction conditions could influence the selectivity toward propene but not the propane consumption TOF, because of the zero-order dependence of the reaction with respect to O_2 partial pressure.[130]

dx.doi.org/10.1021/cs5003417 | ACS Catal. 2014, 4, 3357−3380

Table 5. Summary of Propane ODH Kinetics over Supported V_2O_5/Al_2O_3 Catalysts and Catalyst Properties from Selected Publications

$E_{a\ 1}$ [kJ/mol]	$TOF_{propane}$ [$\times 10^{-3}$ s^{-1}]	temp [°C]	BET [m^2/g]	V_2O_5 [% wt]	V [atom/nm^2]	synthesis method (precursor−solvent)[a]	ref
81		350−500	148−182	5−15	1.8−6.7	IWI (AMV−H_2O)	92
117−120	1.3 (390 °C) 1.8 (400 °C) 26.6 (500 °C)	330−390	95	2	1.4	IWI (AMV−H_2O)	132
	2.7 (400 °C) 41 (500 °C)	500	185	4.8	1.52	IWI (AMV−H_2O)	114
	0.1−1.2 (400 °C) 1−18 (500 °C)	500	109.4−97.5	2.4−12	1.5−8.8	grafting (VAc.−toluene)	129
	1.7 (400 °C) 16 (500 °C)	450−500	186.8	4.0	1.3	IWI (AMV−H_2O)	115
80.3		300−400	141	15.8	4.4	IWI (AMV−H_2O)	133
	0.7−3.6 (400 °C) 5−29 (475 °C) 9−53.3 (500 °C)	400−500	8.7−124	0.9−16.9	0.5−129	grafting (VAc.−toluene)	38
113	6.8 (400 °C) 92.6 (500 °C)	400−500	96	2.1	1.4	grafting (VAc.−toluene)	37
	2.8 (400 °C) 41.1(500 °C)	500	209	4.8	1.5	IWI (AMV−H_2O)	117
	0.1−1.5 (333 °C) 0.9−15.1 (400 °C) 12.7−226 (500 °C)	333	86−100	0.7−15	0.5−7.7	IWI (AMV−H_2O)	118
	1−1.4 (350 °C) 5.1−7.5 (400 °C) 68.8−112 (500 °C)	350		3−20	1−8	IWI (VTiP−2- propanol)	40
87	2.5 (380) 4.6 (400 °C) 63.2 (500 °C)	380−480	258	2	0.9	IWI (AMV−H_2O)	134
	1−9.3 (400 °C) 1.8−18 (430 °C) 7.7−69.3 (500 °C)	430	86−100	0.7−10	0.5−7.7	IWI (AMV−H_2O)	128
111	2.2 (400 °C) 40.4 (500 °C)	400−500	106.6	2.5	1.6	grafting (VAc.−toluene)	130
100−92	3.5−4.9 (380 °C) 6−8.1 (400 °C) 57.6−68 (500 °C)	380	110−165	5−15	2−9	IWI (AMV−H_2O)	135
103	2.5−17.5 (400 °C) 27−190 (500 °C)	310−400	91.1−108.1	3.1−14.8	1.9−10.7	IWI (VTiP−2- propanol)	41
96	1 (380 °C) 1.7 (400 °C) 15.5 (500 °C)	380	146	10	4.5	IWI (AMV−H_2O)	112
	1.5−3.9 (400 °C) 4.7−12.0 (440 °C) 21.7−52.7 (500 °C)	440	8.7−124	0.5−9.5	0.3−72.3	V_2O_5 powder (OA)	131

[a]IWI = incipient wetness impregnation. AMV = ammonium methavanadate. OA = oxalic acid. VAc. = vanadium acetyl acetate. VTiP = vanadium triisopropoxide.

Another difference found in the studies mentioned above is the nature of the Al_2O_3 supports, which originated from different sources. Yang et al.[41] employed Al_2O_3 from Degussa AG (BET = 107 m^2/g) prepared by burning aluminum chloride, whereas Tian et al.[40] used Al_2O_3 from Engelhard (BET = 222 m^2/g) prepared by wet chemistry. Aside from the different BET surfaces areas and due to the different methods employed to prepare the Al_2O_3, differences in the surface chemistry may also be present (e.g., such as residual surface chlorine that may interact with the surface vanadia species).

In comparison to the reducible supports discussed above, the performance of the alumina-supported species is considerably inferior. This allows several conclusions. Either on alumina a different active species exists than on reducible supports, or the reducible supports participate in the action of the catalyst. A more subtle interpretation would be that the same active V_xO_y species functions to a different degree as catalyst that is controlled by the electronic (semiconducting) properties of the support. The redox potential of a metal ion in different ligand environments is well-known to be different (e.g., pH in water) and so may the semiconducting band structure of the wide bandgap support alumina be less beneficial than the more defect-controlled narrowed band structure of the reducible oxides.

Supported V_2O_5/SiO_2 Catalysts. Supported V_2O_5/SiO_2 catalysts are the most studied for propane ODH, as shown by

dx.doi.org/10.1021/cs5003417 | ACS Catal. 2014, 4, 3357−3380

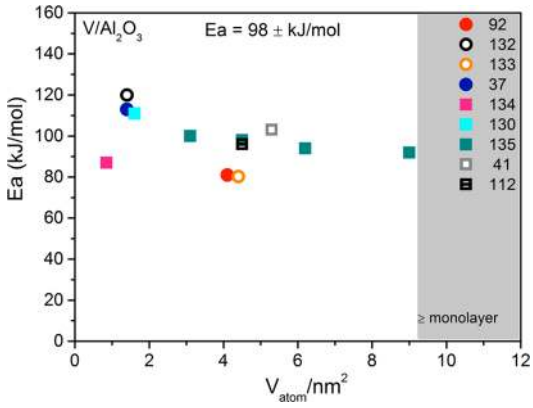

Figure 8. Apparent propane ODH activation energies as a function of vanadia loading on the Al_2O_3 support. The gray region indicates that the experimental monolayer surface vanadia coverage has been exceeded. The numbers indicate the cited references. Open symbols represent recalculated values that are explained in the Supporting Information.

the number of entries in Table 6. Once again, the majority of the V_2O_5/SiO_2 catalysts were prepared by IWI with AMV and H_2O as precursor and solvent, respectively. In some cases, methanol was used instead of H_2O in order to improve the AMV solubility.[34−36,136,137] In many cases, oxalic acid was also added to the aqueous solution to improve the vanadium oxide solubility. In addition, the grafting method has also been used to prepare V_2O_5/SiO_2 catalysts, being the second-most-used methodology. Interestingly, only one publication reported propane ODH kinetics for supported V_2O_5/SiO_2 catalysts prepared by the IWI method using vanadium triisoprpoxide in 2-propanol as precursor and solvent, respectively.[40]

The reported apparent propane ODH activation energy for V_2O_5/SiO_2 catalysts is ∼117 ± 28 kJ/mol (Figure 10). Such a high standard deviation does not reflect the low accuracy in the determination of this parameter but indicates the presence of different catalysts species present in the different investigations. A broad variety of species exist at low loading in accord with the possibility of large spatial freedom, whereas a more space-filling situation creates a homogeneous species. It is also supported by the strong variation of the TOFs as a found for catalysts prepared by different synthesis methods and from different precursors as shown in Figure 11.

In contrast to the other supported vanadium oxide catalysts, there is a wide variation in the reported apparent activation energy values as a function of surface vanadia coverage, oxide support, synthesis method, and the laboratory performing the research. The largest discrepancies in the apparent propane ODH activation energies are observed at low vanadia loadings (<1 V_{atom}/nm^2), and the values asymptotically approach a common value at higher vanadia loadings (>1 V_{atom}/nm^2). Unfortunately, temperature-dependent propane ODH rates at loadings close to monolayer coverage were not found. In light of the observed trend in Figure 10, high vanadium oxide loading seems to minimize the influence of SiO_2 support (with possible impurities) on the overall propane ODH rates.

Schimmoeller et al.[50] reported an apparent propane ODH activation energy of ∼120 kJ/mol over supported V_2O_5/SiO_2 catalyst with the highest vanadia surface density reported so far (∼3.3 V_{atom}/nm^2). Comparable surface vanadia monolayer coverage of ∼2.6 V_{atom}/nm^2 was reported by Gao et al.,[83] but the activation energy was not given. The propane consumption TOFs reported for supported V_2O_5/SiO_2 catalysts as a function of vanadia surface density are presented in Figure 11. Although a broad range of TOFs have been reported, the majority of the TOFs remain relatively constant as a function of surface vanadia coverage. None of the studies reported increasing TOFs as a function of surface vanadia coverage, as found in some studies for supported vanadia catalysts on TiO_2, ZrO_2 , and Al_2O_3. Some of the publications for supported V/SiO_2 catalysts report slight decreases in the propane consumption TOFs with surface vanadia coverage.[35,36,50,146] In situ Raman spectroscopy characterization revealed that the decrease in propane TOF at high vanadia loadings is related to the transformation of the surface vanadia species to V_2O_5 NPs under reaction conditions.[50] Although in situ characterization studies are missing for the majority of the studies, the transformation of the surface vanadia species to V_2O_5 NPs during propane ODH explains the decrease in propane consumption TOF with surface vanadia coverage.

The highest propane consumption TOFs for propane ODH by supported V_2O_5/SiO_2 catalysts were reported by Tian et al.[40] and Schimmoeller et al.[50] (Figure 11). These researchers prepared their catalysts with materials made via pyrolysis of $SiCl_4$: Tian et al.[40] used a SiO_2 support produced via pyrolysis of $SiCl_4$, and Schimmoeller et al.[50] employed FSP to make their supported V_2O_5/SiO_2 catalyst. The common feature of such syntheses is that the resulting oxide supports tend to be very

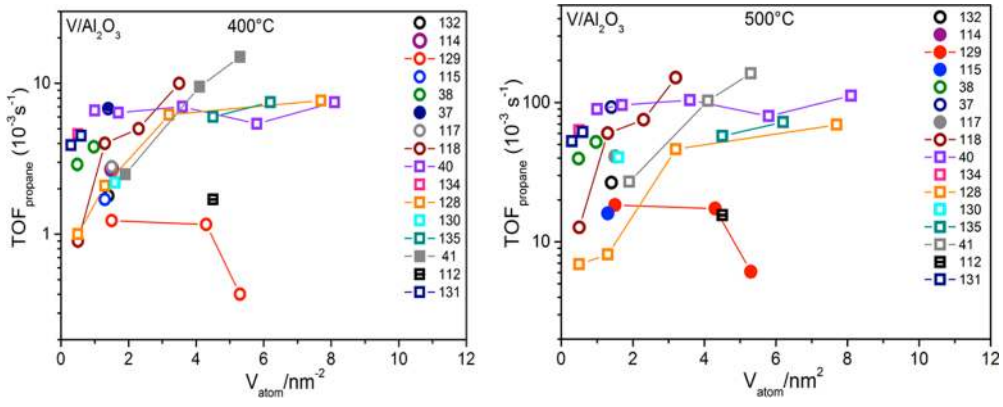

Figure 9. Propane consumption TOF values as a function of surface vanadia coverage over V_2O_5/Al_2O_3 catalysts at (a) 400 and (b) 500 °C. The numbers indicate the cited references. Open symbols represent recalculated values that are explained in the Supporting Information.

dx.doi.org/10.1021/cs5003417 | ACS Catal. 2014, 4, 3357−3380

Table 6. Summary of Propane ODH Kinetics over Supported V_2O_5/SiO_2 Catalysts and Catalyst Properties from Selected Publications

$E_{a\ 1}$ [kJ/mol]	$TOF_{propane} \times 10^{-3}$ s^{-1}]	temp [°C]	BET [m^2/g]	V_2O_5 [% wt]	V [atom/nm^2]	synthesis method (precursor−solvent)[b]	ref
103		400−500		4.8	0.7	IWI (AMV−H_2O)	138
146	1.3 (400 °C) 37.9 (500 °C)	400−500	151	0.6	0.3	grafting (VAc−toluene)	37
	0.4−1.4 (400 °C) 5−17 (475 °C) 10.7−36.3 (500 °C)	400−500	227−892	1.07−20	0.08−25.4	grafting (VAc.−toluene)	38
106−168	0.1−0.3 (400 °C) 0.5−2.6 (450 °C) 1.9−7.3 (500 °C)	425−525	168−281	5.3−50.8	1.3−20	IWI (AMV−H_2O)	139
	0.2 (400 °C) 6 (500 °C)[c]	500	286	5	1.2	IWI (AMV−H_2O)	117
105−141	0.2−0.4 (400 °C) 2.5−11 (500 °C)	425−525	311−746	1.3−14.6	0.09−3.11	IWI (AMV−H_2O)	140
78−158	1.5−1.1 (400 °C) 4−7 (450 °C) 18−23.4 (500 °C)	450−475	790−1059	0.36−9.46	0.02−0.44	grafting VAc.−(toluene) VSul. (water)	39
134−151	0.15−0.23 (400 °C)[a] 3.6−4.3 (500 °C)[a]	380−450	459−118	2.3−13.6	0.6−3.1	grafting (BD- H_2O)	141
	0.1−0.6 (400 °C) 2−16 (500 °C)	500	300−1049	4.8−20	0.4−25.5	grafting (VAc.−toluene)	44
137−168	0.2−0.2 (400 °C) 20−39.6 (550 °C) 5.5−9.2 (500 °C)	450−550	300−820	2.5−10	0.3−1.6	IWI (AMV−methanol)	34
	0.002−0.02(400 °C) 0.9−7.4 (600 °C) 0.1−0.6 (500 °C)	600	222−592	1.8−16	0.2−2.4	IWI (AMV−methanol)	35
	0.005−0.05(400 °C) 1.9−16.1(600 °C) 0.1−1.3 (500 °C)	600	222−985	1.9−16	0.2−2.4	IWI (AMV−methanol)	36
	0.02−0.04 (400 °C) 0.6−1.3 (500 °C) 2.3−5.1 (550 °C)	500−550	181−1113	0.5−1.4	0.03−0.2	IWI (AMV−H_2O)	142
	0.8 (400 °C) 24 (500 °C)	500	790	9.5	0.44	grafting (VAc.−toluene)	45
63−114	0.03−0.2 (400 °C) 0.2−1.7 (500 °C) 0.34−2.4 (520 °C)	425−600	4.5−848	7.2−8.6	0.6−1.6	IWI (AMV−H_2O)	143
	0.2−0.5 (400 °C) 0.01−0.03 (333 °C) 5.2−12.1 (500 °C)	333	251−287	2−15	0.46−4	IWI (AMV−H_2O)	118
	0.28−0.29 (350 °C) 2.1−2.2 (400 °C) 53−54.9 (500 °C)	350		5−12	1.5−2.6	IWI (VTiP−2-propanol)	40
	0.7 (400 °C) 7.1 (500 °C) 43.8 (600 °C)	600	451	8	1.18	IWI (AMV−methanol)	137
35	0.02−0.2 (400 °C) 0.5−5.5 (500 °C) 1.8−22.0 (550 °C)	400−650	448−591	2.5−28.6	0.15−2.40	IWI (AMV−methanol)	136
	0.04−0.1 (400 °C) 0.2−1.8 (500 °C) 0.6−6.8 (550 °C)	550	50−1013	1.1−18.4	0.1−24.4	grafting (VAc.−ethanol)	144
62	5.3−14.7 (400 °C) 22.2−61.1(500 °C)	500	706−1109	1−3.7	0.09−0.35	IWI (AMV−H_2O)	145
	0.3 (400 °C) 6.6 (500 °C)	500	286	5	1.2	IWI (AMV−H_2O)	114
81−126	0.8−2 (400 °C) 5.2−15.3 (500 °C) 11.1−35.3 (550 °C)	400−550	333−119	3−50	0.6−27.6	FSP (AMV)	50
	0.7 (400 °C)	500	413−871	2.7−3.9	0.4−1.1	grafting (VAc.−toluene)	43

dx.doi.org/10.1021/cs5003417 | ACS Catal. 2014, 4, 3357−3380

Table 6. continued

$E_{a\ 1}$ [kJ/mol]	$TOF_{propane} \times 10^{-3}$ s^{-1}]	temp [°C]	BET [m^2/g]	V_2O_5 [% wt]	V [atom/nm^2]	synthesis method (precursor−solvent)[b]	ref
90	20 (500 °C) 1.5−3.6 (400 °C) 12.1−28.8 (500 °C) 41.4−98.9 (575 °C)	500−620	592−819	0.2−1.7	0.02−0.19	MCS (AMV−H_2O)	146

[a]Data provided directly by the authors. [b]IWI = incipient wetness impregnation. VAc. = vanadium acetyl acetate. AMV = ammonium methavanadate. FSP = flame spray pyrolysis. VTiP = vanadium triisopropoxide. BD = butylammonium decavanadate. MCS = miscellaneous catalyst synthesis.

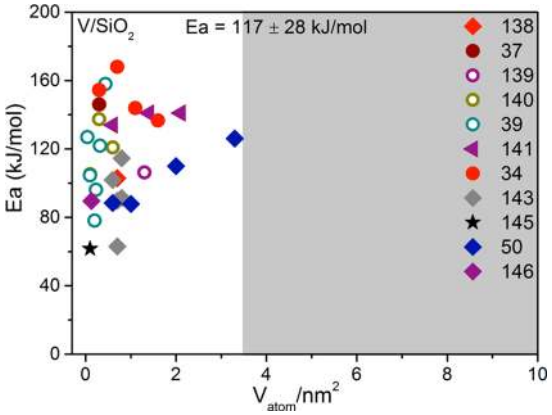

Figure 10. Propane oxidation activation energies as a function of vanadia coverage on the SiO_2 support. The gray region indicates that the experimental monolayer surface vanadia coverage has been exceeded. The numbers indicate the cited references. Open symbols represent the recalculated values that are explained in the Supporting Information.

clean and most probably accounts for these two studies reporting the highest propane ODH TOFs. Despite the catalysts being prepared using different methods (Table 6), both authors concluded that the catalysts showed unique properties in terms of vanadia dispersion. Characterization studies demonstrated that predominantly isolated surafce VO_x species were present in these catalysts up to a relatively high vanadia surface density. Whereas Schimmoeller et al.[50] found that the TOFs decreased with surface vanadia coverage, Tian et al.[40] found that the TOF value was constant with surface vanadia coverage. This difference is most likely related to the milder reaction conditions employed by Tian et al.[40] (350 °C and propane conversions less than 3%) the more aggressive reaction conditions used by Schimmoeller et al.[50] (550 °C and 8.5−25% propane conversion) with the latter possibly leading to transformation of the surface VO_4 sites to crystalline V_2O_5.

Gruene et al.[141] used a grafting/anion exchange procedure to synthesize highly dispersed vanadium oxide catalysts, as high as 3.1 V_{atom}/nm^2 and found that TOFs of propane ODH remained constant with surface vanadia coverage on SiO_2 at 400 and 500 °C (propane conversion bellow 10%). The reported TOFs, however, were about an order of magnitude smaller when extrapolated to 400 and 500 °C.

High propane consumption TOFs were also obtained for supported V_2O_5/SiO_2 catalysts prepared from syntheses not employing the standard aqueous AMV IWI method (see Figure 11 and Table 6). Liu et al.[146] prepared vanadosilicate molecular sieves by sol−gel methodology and established that, despite of this catalysts exhibit higher activity and selectivity for propane ODH than the V-impregned SBA-15 catalysts, the TOFs of propane ODH decreased with surface vanadia coverage. A similar trend (decreasing TOFs) as a function of surface vanadia coverage was also reported by Liu et al.[136] and Vidal-Moya et al.[144] for vanadosilicate molecular sieves. The decreasing TOFs with increasing vanadia loading may very well have been due to agglomeration of dispersed vanadia to crystalline V_2O_5 given the rather high reaction temperature of 550 °C.[50]

The lowest TOFs for supported V_2O_5/SiO_2 catalysts were reported by Fan. et al.[35,36] (see Figure 11). These catalysts were prepared by impregnating SBA-15 with a methanol solution of AMV. Despite the lowest propane consumption TOFs obtained in this work,[35] Cavani's review[12] showed this catalyst system as one of most promising due to the high propene yield. This suggests that a proper comparison of different catalytic results from different research groups should not be done using the typical propene selectivity−propane conversion plots. The absence of characterization for these supported V_2O_5/SBA-15 catalysts does not allow an exact determination of TOF data

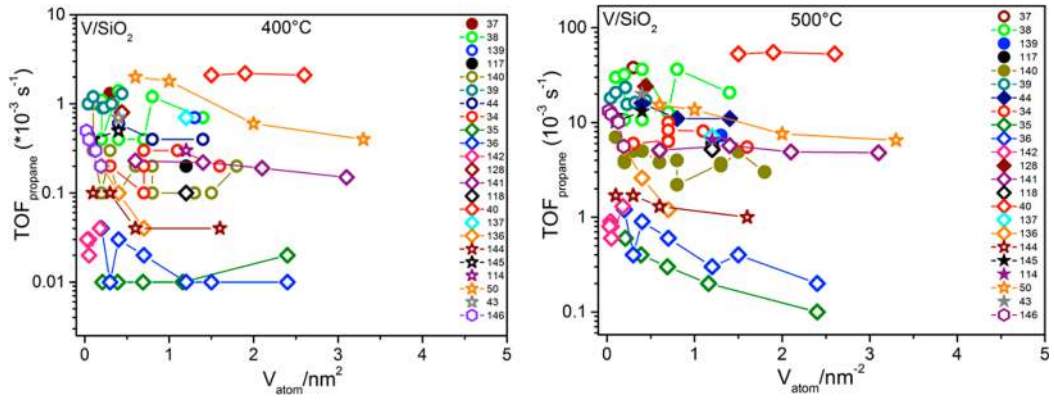

Figure 11. Propane consumption TOFs as a function of surface vanadia coverage over supported V_2O_5/SiO_2 catalysts at (a) 400 and (b) 500 °C. The numbers indicate the cited references. Open symbols represent the recalculated values that are explained in the Supporting Information.

dx.doi.org/10.1021/cs5003417 | ACS Catal. 2014, 4, 3357−3380

due to the presence of large V_2O_5 NPs, V-encapsulation, or surface impurities.

2. STRUCTURE–REACTIVITY RELATIONSHIPS

From the above reviewed propane ODH kinetic data, it becomes apparent that several potential experimental parameters (surface vanadia coverage, oxide support, reaction conditions, etc.) can perturb the propane ODH kinetics data. The apparent propane ODH activation energy (E_a) as a function of vanadia coverage (ML = vanadia monolayer coverage) for supported vanadium oxide catalysts is presented in Figure 12. The error bars represent the standard deviation of the collected data and reflect the discrepancies between the selected studies with respect to purity of materials, precision, and reproducibility of the experiments. The small standard deviations in the activation energies indicate that the majority of the reported kinetic data are in good agreement. The surface vanadium oxide coverage does not considerably alter the activation energy. Only for the supported V_2O_5/TiO_2 catalysts do the activation energies show a slight decrease above half-monolayer surface vanadia coverage. The relatively constant activation energy as a function of surface vanadia coverage reveals that the ratio of surface polymeric/monomeric VO_4 species, which increases with coverage, does not affect the propane ODH mechanism at supported vanadium oxide catalysts.

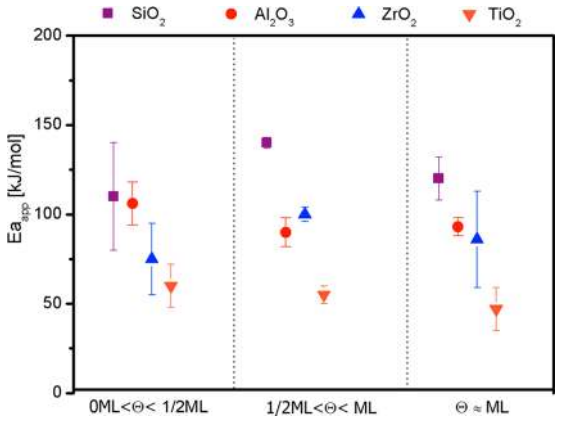

Figure 12. Apparent propane ODH activation energy as a function of surface vanadia coverage as a function of oxide supports. The E_a values represent an average of the reported literature data for each oxide support and the error bars represent the standard deviation.

For supported vanadium oxide catalysts at submonolayer coverage, the apparent propane ODH activation energies vary from 45 to 150 kJ/mol, which reflects the strong support influences on propane ODH kinetics. In addition, the apparent activation energy for supported V_2O_5/NbO_5[147] and V_2O_5/CeO_2[37] catalysts are ~157 and 68 kJ/mol, respectively. The apparent activation energy decreases as follows V_2O_5/NbO_5 > V/SiO_2 > V/Al_2O_3 > V/ZrO_2 > V/CeO_2 > V/TiO_2. The strong influence of the specific oxide support upon the apparent activation energy demonstrates the critical role of the bridging V–O–Support bond in the mechanism and the impact of its strength on the propane ODH reaction kinetics.

The propane consumption TOFs as a function of vanadia coverage for the different oxide supports are presented in Figure 13. The average TOFs calculated from the literature data demonstrate that the TOFs are constant as a function of vanadia coverage. The same constant TOF trend has also been found for the supported V_2O_5/Nb_2O_5 catalysts.[147] The trend of constant TOFs as a function of surface vanadia coverage has recently been confirmed for 100% dispersed surface vanadia on several supports, confirmed by Raman spectroscopy, as shown elsewhere.[119] The constant TOFs with vanadia surface coverage shows that the ratio of surface VO_4 polymers/monomers does not affect the propane ODH kinetics and demonstrates that surface monomers and polymers exhibit the same activity. The specific oxide support, however, has a pronounced effect upon the TOFs reflecting the significant influence of the bridging V–O–Support bond upon propane ODH.[119]

The variation of the TOFs with the specific oxide support has been found to be inversely related to the reducibility, quantified by the maximum temperature of the hydrogen consumption peak (T_{max}) of the supported vanadium oxide catalysts during H_2-TPR.[115] The same inverse trend between TOF and T_{max} was earlier found also for the CH_3OH ODH over supported vanadia catalysts.[148] In fact, the inverse trend between TOF and T_{max} has also been found for numerous other oxidation reactions by supported vanadium oxide catalysts (e.g., CH_3OH, C_2H_6, SO_2).[148−150] This universal trend for oxidation reactions by supported vanadium oxide catalysts has recently been correlated with the oxygen defect formation enthalpy (ΔH_{def}) of the supported vanadia catalysts determined by impedance spectroscopy.[120]

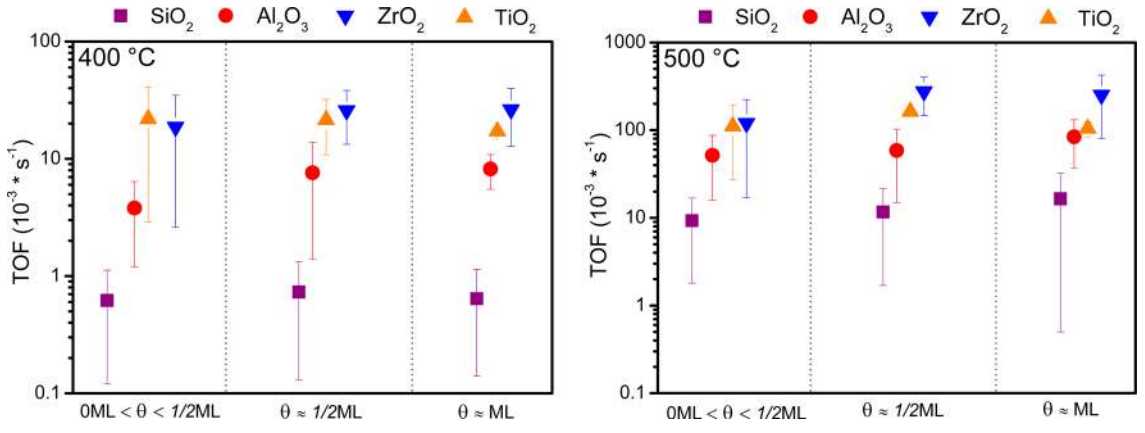

Figure 13. Propane consumption TOF values as a function of surface vanadia coverage as a function of different supports at 400 and 500 °C. The TOF values represent an average of the reported kinetic data, and the error bars represent the standard deviation.

dx.doi.org/10.1021/cs5003417 | ACS Catal. 2014, 4, 3357−3380

Beck et al.[120] found a linear free energy relation between ΔH_{def} and the apparent activation energy of the propane ODH and partial oxidation of ethanol, as shown in Figure 14. The

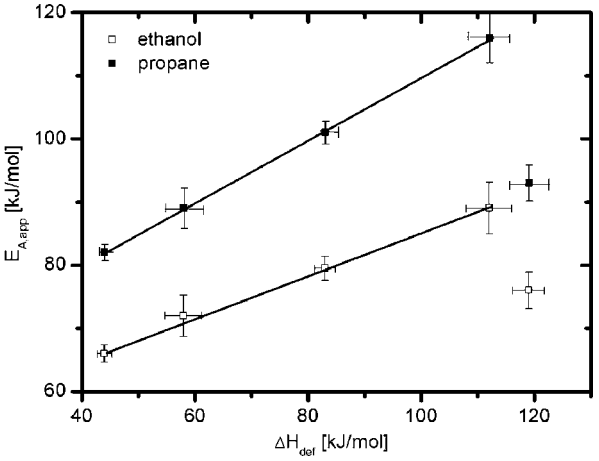

Figure 14. Correlation of defect formation enthalpy with activation energy of propane and ethanol oxidation.[120]

different slopes for propane ODH and ethanol ODH are related to the different C−H bond strengths of the two reactants involved in the rate-determining step. These findings confirm that the reducibility of the supported vanadia species dependent on the strength of the bridging V−O−Support bond, which is the critical parameter controlling the rates of ODH reactions by supported vanadium oxide catalysts.

Although the above review definitively demonstrates that the propane ODH TOF values are independent of surface vanadia coverage, which also indicates the absence of influence of surface vanadia polymer/monomer ratio, it was surprisingly found that crystalline V_2O_5 NPs in the ±1−3 nm range exhibit anomalously high propane ODH TOFs.[119] This new result finally explains the few propane ODH kinetic studies that show increasing propane ODH TOFs with increasing surface vanadia coverage, because those studies employed the poorly soluble AMV precursor and reported the presence of V_2O_5 NPs in their catalysts.

In summary, the isolated and polymeric surface VO_4 species possess the same propane ODH TOFs on the same oxide support. Constant TOF for propane consumption as a function of surface vanadia coverage indicates that only one surface VO_4 site is involved in rate-derterming step of propane activation.[148] Crystalline V_2O_5 NPs in the 1−3 nm range, however, possess anomalously high activity for propane ODH (especially for high C_3/O_2 ratios).[119]

The specific oxide support behaves as a ligand that has a profound effect on the propane ODH kinetics via the bridging V−O−Support bond (ZrO_2 > TiO_2 > Al_2O_3 > SiO_2). These reactivity trends are universal for oxidation reactions by supported vanadium oxide catalysts. This important statement is a clear result of the present analysis and is independent from the exact origin of the effect. It can be generalized that the redox potential of the surface V_xO_y species is a function of the

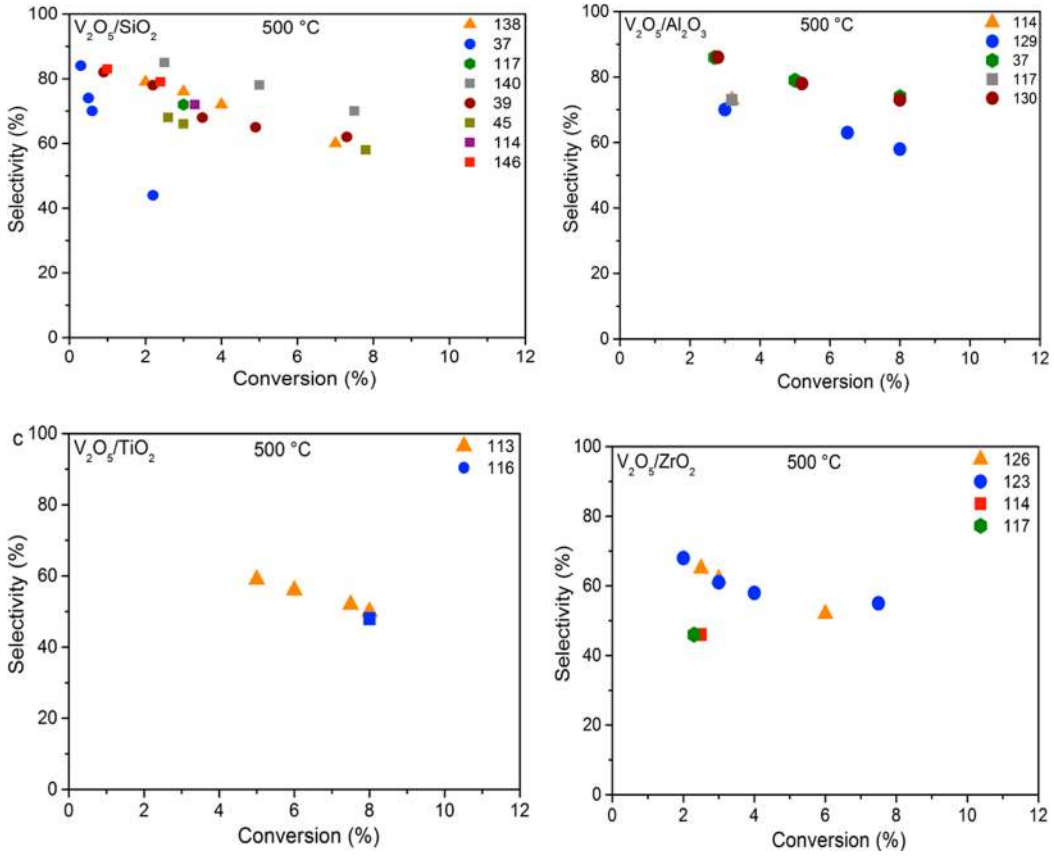

Figure 15. Propane ODH selectivity−conversion trajectories reported for supported V_2O_5 catalysts in the literature. The number inside the square bracket [#] indicates the quoted reference. Catalytic testing was carried out at similar reaction conditions.

dx.doi.org/10.1021/cs5003417 | ACS Catal. 2014, 4, 3357−3380

electronic structure of the support ligand. One of these is the defect formation energy that scales with the band structure of the solid support. This results in a Bronsted−Evans−Polyny relationship between the propane ODH activation energy and the defect formation enthalpy as the scaling parameter.

3. PROPANE ODH SELECTIVITY TOWARD PROPENE

High selectivity toward propene at high propane conversion is a challenge in propane ODH because of propene combustion due to its higher reactivity in comparison to propane. Improving of the selectivity for propene ultimately requires knowledge of the elementary reactions controlling the total oxidation reactions to CO and CO_2.

Highly dispersed surface vanadia species seem the most selective to propene,[12,141,149,151] but such high dispersion is only found for very low vanadia loadings (<2 V/nm^2).[40] The main drawback of the vanadia dispersion is that a decrease of V loading introduces a dependence of selectivity on different factors, such as support nature and acidity.[152]

In order to address the issue of selectivity, the propane ODH reaction network has been extensively studied using periodic density functional theory (DFT). Recently, a DFT analysis on fully oxidized (001) V_2O_5 and V_2O_5/TiO_2 surfaces was reported addressing the issue of selectivity by extending the propane ODH reaction network including the formation of oxygenated products. It was concluded that although the V═O vanadyl oxygen is to be the most active for any type of selective oxidation reaction, the bridging oxygen is more selective toward propane dehydrogenation.[153] Rozanska et al.[154] found that only vanadyl sites are involved in the rate-determining step, but second hydrogen abstraction may occur also at bridging oxygen atom without changing the overall kinetics of the reaction. Unfortunately, this question cannot be clarified by experimental kinetic studies since the rate-determining step is dissociative adsorption of propane and all subsequent steps are too fast to be monitored. On the other hand, Nguyen et al.[155a] concluded that vandyl oxygen sites play the crucial role for all reactions of the propane ODH reaction network. For the total oxidation of propene the rate-determining step is again the C−H activation of the allylic C−H bonds.[155b]

Selectivity−conversion plots can easily be overinterpreted because they eliminate the influence of residence time, mixing characteristics, and feed compositions. Nevertheless, they are very helpful for the comparison of the performance of catalysts that have been studied under the same conditions. The interesting observation gained from the review of various data sets was the fact that the propene selectivity trajectories as a function of propane conversion are quite similar, no matter what support material is used (Figure 15). This indicates that the ratio between the rate constants of the dehydrogenation step and the propene oxidation step has to be roughly the same or can only vary within a small range no matter how active the catalyst is, as will be shown in the next section about kinetic analysis of the reaction network. In addition, the selectivity increases at all catalysts with increasing temperature,[37] indicating that the activation energy of the oxidative dehydrogenation is always higher than that of the total oxidation of propene. Therefore, propane ODH should be performed at a temperature as high as possible, up to a temperature where unselective gas phase reactions can be excluded.

In summary, as is depicted in Figure 13, the support material strongly influences activity of supported vanadia catalysts for propane ODH while very similar selectivity−conversion trajectories are observed over different support materials (Figure 15). The different TOFs (Figure 13) of the supported vanadia catalysts with respect to the oxide support imply that the specific oxide support influences the Arrhenius pre-exponential factors for both, the dehydrogenation step (r_1) and the consecutive propene combustion reaction (r_2) in the same way because the formation of the transition state of the rate-determining step is favored for the more easily reduced catalysts. Therefore, the selectivity of a supported vanadia catalyst with a single support material cannot be altered.

A thorough kinetic analysis of the propene selectivity during propane ODH would require a correct reaction network for the overall process up to the formation of CO and CO_2. As this reaction network is far more complex than the usual kinetic triangle, care must be taken in a superficial discussion found in the literature and reported here. This is illustrated by the fact that combustion requires besides C−H activation also the C−C bond breaking which hardly can occur on a site activating C−H bonds.

In addition, combustion also requires as a first step the abstraction of a proton that implies that a common reaction intermediate (C_3H_7*) that links reaction channels to combustion and oxidative dehydrogenation, and the selectivity is decided after the initial C−H abstraction. The extinction of support effects in the desired exit channel of the reaction network and the finding of strong support effects in the entry channel to the reaction network may be rationalized by the assumption that the reaction does not proceed on one and the same active site but that by an initial step the activated radical C_3H_7* is formed, and its consecutive reaction is controlled by different active sites accepting the activated propane.

3. OVERALL PROPANE ODH REACTION KINETICS

The oxidative dehydrogenation of propane to propene over supported vanadia catalysts has been found to be first-order with respect to propane partial pressure and zero-order with respect to molecular O_2 partial pressure, which suggests that the rate-determining step involves C−H activation of propane.[56,91,130,132,138,154−157] This is supported by isotope labeling experiments which also indicate that the rate-determining step involves C−H bond breaking of the CH_2 functionality with the weaker C−H bond strength than the terminal CH_3 groups.[157] Furthermore, isotopic labeling experiments with C_3H_8/C_3D_8 have also shown that the intitial H-abstraction step is irreversible.[158] The zero-order dependence of the propane ODH reaction with respect to molecular O_2 indicates that reaction kinetics are independent of O_2 partial pressure and is consistent with the finding that reoxidation of the supported vanadia catalyst occurs much faster than propane oxidation (by ~10^5 times).[159] This suggests that the participating surface vanadia species are fully oxidized during propane ODH.[23]

The overall propane ODH kinetics for propane consumption can be described by the MvK rate law (eq 1):

$$r_{C_3H_8} = \frac{1}{\frac{1}{k_{red}[P_{C_3H_8}]} + \frac{1}{k_{ox}[P_{O_2}]}} \quad (1)$$

This kinetic expression can be further simplified because of the much faster reoxidation step $1/k_{ox}[P_{O_2}]$ than the propane reduction step $1/k_{red}[P_{C_3H_8}]$ as shown in eq 2:

dx.doi.org/10.1021/cs5003417 | ACS Catal. 2014, 4, 3357−3380

$$r_{C_3H_8} = k_{red}[P_{C_3H_8}] \quad (2)$$

This simplified kinetic expression is equivalent to a power law approach (eq 3) for zero-order dependence on molecular O_2 with the exponents $n1 = 1$ and $m1 = 0$.[138]

$$r_1 = k\exp\left(\frac{-E_a}{RT}\right)C_{C_3H_8}^{n^1}C_{O_2}^{m^1} \quad (3)$$

Selectivity-conversion plots[37] have shown that the intercept of the trajectory at the selectivity axis is nearly 100%, which indicates that the consecutive total oxidation of propene to CO_x is the predominant side-reaction that determines the selectivity toward propene. Thus, the overall kinetic expression for propylene production is given by eq 4.

$$r_{C_3H_8} = k_1 p_{C_3H_8}^1 p_{O_2}^0 - k_2 p_{C_3H_6}^1 p_{O_2}^0 \quad (4)$$

The above propane ODH kinetic expression indicates that direct propane combustion is negligible. Only a few authors have determined the kinetic parameters of both reactions as shown in Table 7. For all materials apparent propane ODH

Table 7. Pre-Exponential Factors (k_{1oo}) and Apparent Activation Energy (E_{a_1}) for Propane Dehydrogenation, As Well As Apparent Activation Energy ($E_{a_2,\ app}$) and Pre-Exponential Factors (k_{2oo}) for Propene Combustion

	TiO_2		ZrO_2	Al_2O_3		SiO_2
k_{1oo} (mL/min·g)	87	189		48	17	2.2[a]
k_{2oo} (mL/min·g)	1488	2275		574	230	700
$E_{a_1,\ app}$ (kJ/mol)	65	54	99	81	96	103
$E_{a_2,\ app}$ (kJ/mol)	47	26	51	39	58	34
ref	112	92	127	92	112	138

[a] $\times 10^6$.

activation energies are higher than for propene combustion. Higher pre-exponential factors for propene combustion are observed for all materials except for SiO_2 resulting in the highest k_1/k_2 ratio in comparison to the other catalysts.

The apparent activation energies of k_2 (values in line 4 of Table 7) have been found to be lower than the apparent activation energy of k_1 (values in line 3 of Table 7) by about 40 kJ/mol. This difference essentially corresponds to the difference in the weakest C−H bond energies present in propane and propene (401 and 361 kJ/mol, respectively).[127] A specific support effect cannot be derived from such C−H bond strength relationships.

For the discussion of this apparent kinetic, parameters need to be split up into the contributions. For the apparent activation (eq 5), this is the intrinsic activation energy and heat of adsorption.

$$\Delta E_{app} = \Delta E_I + \Delta H_{ads} \quad (5)$$

The heat of adsorption was determined experimentally as a function of exposure for a V_xO_y system on silica, and a value of ~40 kJ/mol was found for a small number of about 10^{16} sites/m^2.

From transition state theory the pre-exponential factors can be expressed as

$$A_1 = (k_B T/h)\exp[(\Delta S_I^{ads} + \Delta S_{II}^r)/R] \quad (6)$$

which essentially considers the entropy change due to reactants adsorption in the formation of the transition state.

Additional molecular details about propane ODH by supported vanadia catalysts cannot be experimentally accessed because the rate-determining step is C−H activation of propane and, consequently, all subsequent elementary reaction steps occur much faster than the rate-determining step.

The fact that the reducibility is responsible for the support effect is supported not only by the mentioned empirical findings but also by theoretical studies based on the energy of hydrogenation as well as the oxygen defect formation energy as reactivity descriptors for C−H activation catalysts.[170,171] Selective oxidation reactions have already been studied theoretically on gas-phase vanadium oxide species,[160,161] on supported catalysts with vanadia coverage below the monolayer,[154,162−165] at the monolayer,[153] and on the (001) V_2O_5 surface.[155a,156−167]

These studies need to be extended before to the selective determining elementary steps before conclusions can be drawn about the rational design of a catalytic material with substantially higher selectivity for propene.

4. CONCLUSIONS

The careful refinement of a large pool of experimental data that apparently present a complex interaction in a multi parameter space results in a surprisingly simple picture of this family of monolayer catalyst that is controlled by only one scaling parameter. This is the energy of the formation of oxygen defects at the vanadia-covered surface that expresses the reducibility of the active site by the reactant. This atomistic picture is the result of several approximations. In generalized form, the scaling parameter is the redox potential of the active site that is a function of the nature of the V_xO_y species plus a strong contribution from the electronic structure of the support. If we assume the active site to be of the same structure on all supports that is justified at least for the limiting of approaching monolayer coverage then the activity in propane activation is a function of the support times a constant.

This parameter influences all reactions involved in the reaction network of the oxidative dehydrogenation of propane in the same way, resulting in a very similar selectivity at all catalysts. This is an unexpected result because activity of the catalysts varies by about 3 orders of magnitude with a variation of the support material. For all monolayer catalyst the kinetics of the propene formation can be described by a simple rate expression that is first order in propane for the propene formation as well as first order in propene for the propene deep oxidation. Both rates are independent of the partial pressure of oxygen, which is an indication of a fast reoxidation of the catalytic sites. No further elementary step can be resolved in experimental kinetic studies because the rate-determining step for both reactions is the activation of the first C−H bond. This required theoretical reaction path analysis for further elucidation of the reaction mechanism. For instance, recently, a reaction path analysis of propane selective oxidation over V_2O_5 and V_2O_5/TiO_2 by using periodic density functional theory (DFT) has been reported.[153] The most favorable reaction pathways for propane ODH is the activation of propane via hydrogen abstraction from the methylene C−H bond. Propane chemisorption occurs via a rebound mechanism, but only its hydrogen abstraction step is required for propene formation. Also, deep oxidation reactions in the propane ODH has been studied by using the periodic DFT method.[168]The

dx.doi.org/10.1021/cs5003417 | ACS Catal. 2014, 4, 3357−3380

authors concluded that starting from the isopropoxide intermediate, there are two competitive reaction pathways leading to the formation of the product propene and byproduct acetone. Both propene and acetone can be completely oxidized to CO_2 but oxygen bridging sites on V_2O_5 (001) are inert for both acetone formation from isopropoxide and further oxidations of acetone and propene indicating that oxygen bridging sites are crucial for propene selectivity, implying that highly dispersed VO_x species are desired. The above-mentioned DFT studies depict a rational mechanism pathway for propene formation in propane ODH which are in agreement with the experimental propane ODH kinetic data summarized in this review.

The kinetic parameters obtained from the reviewed experimental investigations can be summarized in the following reaction energy profile that is calculated for the energy changes per active site over V_2O_5/Al_2O_3 catalysts (Figure 16).

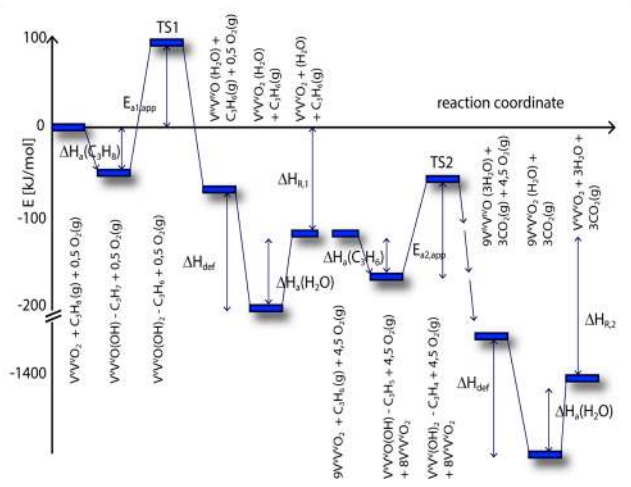

Figure 16. Energy profile for propane ODH (left) and rate-determining step of propene combustion over VO_x/Al_2O_3 catalysts.

In the first step of the profile that represents the propane ODH, only one site is involved to provide one oxygen atom for the formation of one molecule of water. The deep oxidation of propene requires nine oxygen atoms from the catalyst surface in order to produce three molecules of water and the molecules of carbon dioxide. Because the first hydrogen abstraction is the most demanding step, it controls the rate of the complete step. Additionally, every oxygen atom consumed produces the same defect that needs to be reoxidized. For this reason, only the first hydrogen abstraction from propene is shown in the profile. All further steps happen in parallel at different vanadia sites of the catalyst and add up to the overall reaction enthalpy of the propene combustion.

Many parameters of the catalyst preparation and the kinetic investigations can cover this simple relationship between catalyst properties and performance:

1. The catalyst synthesis procedure and vanadia loading are critical in determining the distribution between isolated surface VO_4 sites, polymeric surface VO_4 sites, V_2O_5 NPs on oxide supports, and encapsulation of VO_x sites inside the support lattice.
2. The nature of the oxide support is critical because (i) surface impurities can affect the structure and reactivity of the surface VO_4 sites and (ii) thermal instability can lead to sintering and encapsulating of the active surface VO_4 sites.
3. The oxide support has a pronounced effect on the specific propane ODH activity of surface VO_4 sites and affects characteristics of the surface VO_4 sites via the bridging V−O−Support bond.
4. The bridging V−O−V bonds have a negligible effect on the specific propane ODH activity of surface VO_4 sites because isolated and polymeric surface sites possess the same TOF values on the same support.
5. The V_2O_5 NPs, ∼1−3 nm, possess anomalously high propane ODH reactivity for $C_3/O_2 \gg 1$.
6. Some preparation methods result in an undefined distribution of vanadia on the surface and in the bulk of the support material that allows no exact calculation of active sites.
7. The huge activity difference leads to different experimental conditions for the catalytic experiments. The more active catalysts are usually tested at much lower temperatures than the less active ones.

Results obtained from such different preparation procedures and test conditions have led to increased complexity. The boundary conditions of the propane ODH are set by the involved molecules themselves. The higher reactivity of propene that causes a rate constant for the deep oxidation reaction will always be higher than that of the dehydrogenation reaction. It results in a maximum yield of propene substantially below 100%. For monolayer catalysts, the only option for achieving this maximum yield is the operation of the reaction at the highest possible temperature, where no unselective gas-phase reactions occur. If this is combined with a short contact time reactor, a reasonable space−time yield may be obtained. However, only few efforts have been taken to realize this potential by the construction of an appropriate microreactor.[172]

For a further improvement, new catalysts need to be developed that show one essential difference in the above shown energy profile. In order to avoid the propene deep oxidation the readsorption needs to be suppressed. It can be done by minimization of the concentration of Lewis acid sites as well as coupling surface-catalyzed activation of propane with gas-phase radical-chain reactions.[169] The studies at monolayer catalysts show a stronger interaction of the stronger Lewis acidic catalyst material with propene than the least Lewis acidic silica support material. This advantage of the silica support is difficult to utilize, because it shows the worst reducibility and with this the lowest activity.

In general, it became clear that one single scaling parameter for an assumed geometry of an active site determines the trend of its activity in forming the activated propane molecule. This is the redox potential of the support. It is puzzling that this dependency on the scaling parameter cannot be found when looking at the kinetics of the desired propene formation, and this indicates that the assumption that one single active site achieves the whole transformation may not be valid. It is likely that the initial C−H activation is the difficult bottleneck and that the resulting highly activated intermediate propyl can convert to propene on other sites with a low specific activity preventing also the overoxidation of propene.

Such a scenario is likely if the initial active site in indeed a monomeric VO_4 site that can only accept one electron. Its reoxidation is only facile if the site can condense to a oligomer to transfer electrons to an oxygen molecule or if a conduction

dx.doi.org/10.1021/cs5003417 | ACS Catal. 2014, 4, 3357−3380

band in the support transports the electrons away to special oxygen activation sites (this being the more likely suggestion). The fact that only a small fraction of vanadia can be determined from a microcalorimetric titration[138] indicates that not every VO_4 unit is suitable but only a minority species—possibly with a frustrated metal−oxygen local geometry. This was recently verified with Mo_xO_y species on silica, where also about 1% of the sites were found to be active and frustrated in local geometry[81] in surprising similarity to vanadia on silica.

The resulting oxygen atoms should be strongly bound to the ubiquitous weakly active vanadia sites where they can form water. In such a picture, the quantity "defect energy" is an indicator for the average redox potential of these ubiquitous sites and does not represent the atomic descriptor for the site activating the propane. The abundance of this second site should be large and may be correlated with the observation of such species by quantitative pulse EPR.[2]

If we assume the interplay of two sites, where one highly active site is diluted and isolated by the second weakly active site on the selective oxidative dehydrogenation process, then there is a significant potential for catalyst modification. We can optimize the chemical potential of the initial active sites to become as active as possible. This can be done by facilitating desorption of propyl, which requires a maximum retention of the withdrawn electron at the active site. This can be tuned by optimizing the coupling of the vanadia site to the conduction band. On the other hand, tuning the metal oxygen bond strength can optimize the maximum abundance of the initial form of the site to activate a C−H bond. This is achieved globally by the redox potential of the support and locally by the right nonrelaxed "frustrated" geometry. Such geometries are only adopted when all relaxed sites are filled and will thus occur in qualitative agreement with experimental observation[58] only when the defect sites of the support need to be used for anchoring V_xO_y.

From this point of view, we would use the defect energy proxy as a measure for the frequency of occurrence of support sites producing frustrated vanadia species. The proxy would become a structural descriptor rather than an electronic one. From solid-state theory aspects, we can state that both functions in catalysis are linked, as low defect formation energies and the availability of charge carriers for polarizing V−O−Support bonds may well go together. From the catalytic function, it may be concluded that the same vanadia species in frustrated form performs the first C−H activation and the dominating same species without geometric frustration will perform the second C−H activation and recombine the $[H^+e^-]$ with preactivated oxygen to water.

From a material science view, it may be desirable to generate more complex support structures exhibiting optimized redox properties as bulk phase in comparison to the supports discussed in the present paper. The trend in Figures 12 and 13 clearly shows that reducible supports are desirable. Self-supporting on the other hand is clearly not a good solution, as then the redox activity of the support is too large, destroying the "site isolation" in the sense that the organic molecule initiates bulk reduction of the oxide in a type of "blast furnace" chemistry where no chance for reoxidation exists. Typical supports are thus ternary oxides between early transition metal species exhibiting low Broensted acidity to avoid olefin chemistry and tunable redox activity between that of titania and that of vanadia.

The loading of the support should be close to a monolayer without critically avoiding three-dimensional particles. Then an optimum of stability and a maximum of frustrated species can be achieved. This is also consistent[58] with experimental observations.

Having selected the phase correctly it is important to tailor its nanostructure such that an optimum of defect sites exists at the surface. Here clusters need to be avoided, because large active sites with multiple strong C−H activation may inhibit the selectivity in the same way as a too low redox potential of the bulk phase.

The design issue gets further complicated by having to observe hydrothermal stability of the defects in order to avoid clustering of the vanadia species which not only leads to the loss of activity but also can quickly damage the selectivity and is thus doubly detrimental. Here promotion comes into play as nonredox-active species may help to stabilize lattice defects at the surface.

Kinetic measures such as optimizing the space velocity carefully for each chemical composition of a supported catalyst also hold promise for optimization. The correct formulation of the catalyst observing gas flow homogeneity and strict avoidance of hot spots when operating at the desired upper limit of the heterogeneous regime of the reaction is further a useful recommendation. Finally schemes of adding sufficient oxygen to guarantee the chemical potential of the catalyst to remain sufficiently high at the few sites that activate propane is another element of kinetic optimization.

As none of these combined measures have been observed in any of the studies reviewed here, it is fair to say the potential of ODH of propane is not exploited yet. Also the potential of monolayer grafted systems is not exploited fully yet and little has been done with regard to enhancements and taking care of the macrokinetic optimization in this respect. The present work thus may be used as a concept for further synthetic work. The authors of this review used the lessons learned here for the preparation of catalysts with a mixed VO_x-TiO_x-monolayer on SBA-15 as support material. The SBA-15 support provides a high specific surface area for a high loading of the active surface vanadia component, whereas the titania improves its reducibility. This results in a highly active catalyst that achieves a space−time yield of more than 6 kg propene per kg catalyst/hour. The propane ODH selectivity, however, is not improved for this catalyst system because the adsorption properties of propane and propene seem to be still in the same relation.[58,173] Further work should be accompanied by a suitable regime of analytical experimentation focusing not only on the nuclearity of the molecular species but also (and with the same level of resolution) on the chemical potential of the metal−oxygen bonds beyond (e.g., frequency shifts in Raman spectra). Such techniques[60b] are still largely unexplored when we remember that the critical active species are only abundant as a minority of a few percent at best. If this comparative review can excite the imagination of catalyst chemists to explore the phase space of grafted catalyst more systematically than done so far it would have served the purpose of analyzing the many reports already existing on the subject.

■ ASSOCIATED CONTENT

Ⓢ Supporting Information

Summary of calculations and assumptions needed for comparison of the data, apparent activation energies, and

dx.doi.org/10.1021/cs5003417 | ACS Catal. 2014, 4, 3357−3380

parameters used in the comparisons. This material is available free of charge via the Internet at http://pubs.acs.org.

AUTHOR INFORMATION

Corresponding Author

*E-mail: ccarrero@chem.wisc.edu.

Present Address

[#](C.A.C.) University of Wisconsin-Madison, Department of Chemistry, 1101 University Avenue, Madison, Wisconsin 53706, United States.

Notes

The authors declare no competing financial interest.

ACKNOWLEDGMENTS

We want to express thanks for the privilege of many inspiring discussions with A. Trunschke and her team. The opportunity to collaborate within the BASCAT team and with F. Rososwski is gratefully acknowledged. Additionally, we specially thank Prof. K.-P. Dinse (Free University, Berlin), Dr. Olga Ovsitser (TU-Berlin), Dr. A. Dinse (BP North America, Illinois), and C. Keturakis (Lehigh University, Pennsylvania) for helpful discussions. This work was mainly supported by the German Research Foundation through the cooperative research center, "Structure, dynamics, and reactivity of transition metal oxide aggregates" (SFB 546, http://www.chemie.hu-berlin.de/sfb546). Also, Dr. Carlos Carrero shows gratitude to the Fundayacucho (Venezuela) − DAAD (Germany) PhD's program for basic funding. The contribution of Professor I.E. Wachs was supported by Department of Energy-Basic Energy Sciences (Grant No. FG02-93ER14350).

REFERENCES

(1) (a) Derouane, E.; Parmon, V.; Lemos, F.; Ribeiro, F. *Sustainable Strategies for the Upgrading of Natural Gas: Fundamentals, Challenges, and Oppportunities*; Springer: Netherlands, 2003. (b) Plotkin, J. S. *Catal. Today* **2005**, *106*, 10−14. Burrington, J. D.; Kartizek, C. T.; Grasseli, R. K. *J. Catal.* **1984**, *87*, 363−380. Grasselli, R. K.; Oku, N.; Seo, T. Sumitomo Chem: Japan. U.S. Patent 6,646,138, 2003.

(2) Chemical Engineering. Making Propylene on-purpose. http://www.che.com/news/Making-propylene-on-purpose_11356.html. (Accessed April 20, 2013).

(3) University of York. The Essential Chemical Online: Propene. http://www.essentialchemicalindustry.org/chemicals/propene.html (accessed August 5, 2013).

(4) Buonomo, F.; Sanfilippo, D.; Trifiro, F.; Ertl, G.; Knözinger, H.; Weitkamp, J. *Handbook of Heterogeneous Catalysis*; Wiley-VCH: Weinheim, 1997; Vol. 5, pp 2140−2151.

(5) Frank, B. *Contributions to a Microkinetic Understanding of the Steam Reforming of Methanol (SRM) and the Oxidative Dehydrogenation of Propane (ODP)*, Ph.D. Thesis, Technical University of Berlin, Berlin, Germany, 2007.

(6) Dinse, A. *New Insights into the Oxidative Dehydrogenation of Propane and Ethane on Supported Vanadium Oxide Catalysts*, Ph.D. Thesis, Technical University of Berlin, Berlin, Germany, 2009.

(7) Lin, M. M. *Appl. Catal., A* **2001**, *207*, 1−16.

(8) Banares, M. A. *Catal. Today* **1999**, *51*, 319−348.

(9) Madeira, L.; Portela, M. *Catal. Rev.-Sci. Eng.* **2002**, *44*, 247−286.

(10) Grzybowska-Swierkosz, B. *Top. Catal.* **2000**, *11*, 23−42.

(11) Grabowski, R. *Catal. Rev.* **2006**, *48*, 199−268.

(12) Cavani, F.; Ballarini, N.; Cericola, A. *Catal. Today* **2007**, *127*, 113−131.

(13) Mars, P.; Van Krevelen, D. W. *Eng. Sci.* **1954**, *3*, 41−57.

(14) Weckhuysen, B. M.; Keller, D. *Catal. Today* **2003**, *78*, 25−46.

(15) Trifiro, F.; Grzybowska, B. *Appl. Catal., A* **1997**, *157*, 195−221.

(16) Hagen, J. *Industrial Catalysis, A Practical Approach*, 2nd ed.; Wiley-VCH: Weinheim, 1999.

(17) Rase, H. F. *Handbook of Commercial Catalysis*; CRC: New York, 2000.

(18) Amiridis, M. D.; Wachs, I. E.; Deo, G.; Jehng, J. M.; Kim, D. S. *J. Catal.* **1996**, *161*, 247−253.

(19) Nobbenhuis, M.; Baiker, A.; Barnickel, P.; Wokaun, A. *Appl. Catal.* **1992**, *85*, 157−172.

(20) Cavani, F.; Trifiro, F.; Jiru, P.; Habersberger, K.; Tvaruzkova, Z. *Zeolites* **1988**, *8*, 12−18.

(21) Herman, R.; Sun, Q.; Shi, C.; Klier, K.; Wang, C.; Hu, H.; Wachs, I. E.; Bhasin, M. *Catal. Today* **1997**, *37*, 1−14.

(22) Bond, G.; Tahir, S. *Appl. Catal.* **1991**, *71*, 1−31.

(23) (a) Frank, B.; Fortrie, R.; Hess, C.; Schlögl, R.; Schomäcker, R. *Appl. Catal., A* **2009**, *353*, 288−295. (b) Goodrow, A.; Bell, A. T.; Head-Gordon, M. *J. Phys. Chem. C* **2009**, *113*, 19361−19364.

(24) Stark, W. J.; Wegner, K.; Pratsinis, S. E.; Baiker, A. *J. Catal.* **2001**, *197*, 182−191.

(25) Rossetti, I.; Fabbrini, L.; Ballarini, N.; Oliva, C.; Cavani, F.; Cericola, A.; Bonelli, B.; Piumetti, M.; Garrone, E.; Dyrbeck, H.; Blekkan, E. A.; Forni, L. *J. Catal.* **2008**, *256*, 45−61.

(26) Schimmoeller, B.; Schulz, H.; Ritter, A.; Reitzmann, A.; Kraushaar-Czarnetzki, B.; Baiker, A.; Pratsinis, S. E. *J. Catal.* **2008**, *256*, 74−83.

(27) Poelman, H.; Sels, B. F.; Olea, M.; Euringer, K.; Paul, J. S.; Moens, B.; Sack, I.; Balcaen, V.; Bertinchamps, F.; Gaigneaux, E. M.; Jacobs, P. A.; Marin, G. B.; Poelman, D.; DeGryse, R. *J. Catal.* **2007**, *245*, 156−172.

(28) Keranen, J.; Carniti, P.; Gervasini, A.; Iiskola, E.; Auroux, A.; Niinisto, L. *Catal. Today* **2004**, *91*, 67−71.

(29) Rice, G.; Scott, S. *J. Mol. Catal. A: Chem.* **1997**, *125*, 73−79.

(30) Gordon, R.; Scott, S. *Langmuir* **1997**, *13*, 1545−1551.

(31) Inumaru, K.; Misono, M.; Okuhara, T. *Appl. Catal., A* **1997**, *149*, 133−149.

(32) (a) Wachs, I. E.; Weckhuysen, B. M. *Appl. Catal., A* **1997**, *157*, 67−90. (b) Mitra, B.; Wachs, I. E.; Deo, G. J. *Catal.* **2006**, *240*, 151−159. (c) Deo, G.; Wachs, I. E. *J. Catal.* **1994**, *146*, 335−345. (d) Wang, X.; Wachs, I. E. *J. Catal.* **2004**, *96*, 211−222.

(33) Schwarz, J.; Contescu, C.; Contescu, A. *Chem. Rev.* **1995**, *95*, 477−510.

(34) Liu, Y. M.; Feng, W. L.; Li, T. C.; He, H. Y.; Dai, W. L.; Huang, W.; Cao, Y.; Fan, K. N. *J. Catal.* **2006**, *239*, 125−136.

(35) Liu, Y. M.; Cao, Y.; Yi, N.; Feng, W. L.; Dai, W. L.; Yan, S. R.; He, H. Y.; Fan, K. N. *J. Catal.* **2004**, *224*, 417−428.

(36) Liu, Y. M.; Cao, Y.; Zhu, K. K.; Yan, S. R.; Dai, W. L.; He, H. Y.; Fan, K. N. *Chem. Commun.* **2002**, *23*, 2832−2833.

(37) Dinse, A.; Frank, B.; Hess, C.; Habel, D.; Schomäcker, R. *J. Mol. Catal. A: Chem.* **2008**, *289*, 28−37.

(38) Kondratenko, E.; Cherian, M.; Baerns, M. *Catal. Today* **2006**, *112*, 60−63.

(39) Kondratenko, E.; Cherian, M.; Baerns, M.; Su, D.; Schlögl, R.; Wang, X.; Wachs, I. E. *J. Catal.* **2005**, *234*, 131−142.

(40) Tian, H.; Ross, E. I.; Wachs, I. E. *J. Phys. Chem. B* **2006**, *110*, 9593−9600.

(41) Yang, S.; Iglesia, E.; Bell, A. T. *J. Phys. Chem. B* **2005**, *109*, 8987−9000.

(42) Gao, X.; Jehng, J. M.; Wachs, I. E. *J. Catal.* **2002**, *209*, 43−50.

(43) Ovsitser, O.; Cherian, M.; Brückner, A.; Kondratenko, E. *J. Catal.* **2009**, *265*, 8−18.

(44) Ovsitser, O.; Cherian, M.; Kondratenko, E. *J. Phys. Chem. C* **2007**, *111*, 8594−8602.

(45) Ovsitser, O.; Kondratenko, E. *Catal. Today* **2009**, *142*, 138−142.

(46) Wang, Y.; Zhang, Q.; Ohishi, Y.; Shishido, T.; Takehira, K. *Catal. Lett.* **2001**, *72*, 215−219.

(47) Wegener, S. L.; Marks, T. J.; Stair, P. C. *Acc. Chem. Res.* **2011**, *45*, 206−214.

(48) Sokolowski, M.; Sokolowska, A.; Michalski, A.; Gokieli, B. *J. Aerosol Sci.* **1977**, *8*, 219−230.

(49) Mädler, L.; Kammler, H.; Mueller, R.; Pratsinis, S. *J. Aerosol Sci.* **2002**, *33*, 369−389.
(50) Schimmoeller, B.; Jiang, Y.; Pratsinis, S.; Baiker, A. *J. Catal.* **2010**, *274*, 64−75.
(51) Schimmoeller, B.; Schulz, H.; Ritter, A.; Reitzmann, A.; Kraushaar-Czarnetzki, B.; Baiker, A.; Pratsinis, S. *J. Catal.* **2008**, *256*, 74−83.
(52) Mueller, R.; Mädler, L.; Pratsinis, S. *Chem. Eng. Sci.* **2003**, *58*, 1969−1976.
(53) Deo, G.; Turek, A. M.; Wachs, I. E.; Machej, T.; Haber, J.; Das, N.; Eckert, H.; Hirt, A. M. *Appl. Catal., A* **1992**, *91*, 27−42.
(54) Roozeboom, F.; Mittelmeijer-Hazeleger, M. C.; Moulijn, J. A.; Medema, J.; De Beer, V. H. J.; Gellings, P. J. *J. Phys. Chem.* **1980**, *84*, 2783−2791.
(55) Sanati, M.; Andersson, A.; Wallenberg, L.; Rebenstorf, B. *Appl. Catal., A* **1993**, *106*, 51−72.
(56) Khodakov, A.; Yang, J.; Su, S.; Iglesia, E.; Bell, A. *J. Catal.* **1998**, *177*, 343−351.
(57) Steinfeldt, N.; Müller, D.; Berndt, H. *Appl. Catal., A* **2004**, *272*, 201−213.
(58) Hamilton, N.; Wolfram, T.; Müller, G. T.; Hävecker, M.; Krönnert, J.; Carrero, C.; Trunschke, A.; Schlögl, R. *Catal. Sci. Technol.* **2012**, *2*, 1346−1359.
(59) Weckhuysen, B. M.; Van Der Voort, P.; Catana, G. *Spectroscopy of Transition Metal Ions on Surfaces*; Leuven University Press: Belgium, 2000.
(60) (a) Jackson, S.; Hargreaves, J. *Metal Oxide Catalysis*; Wiley-VCH: Weinheim, 2009;. (b) Dinse, A.; Wolfram, T.; Carrero, C.; Schlögl, R.; Schomäcker, R.; Dinse, K. P. *J. Phys. Chem. C* **2013**, *117*, 16921−16932. (c) Dinse, A.; Carrero, C.; Ozarowski, A.; Schomäcker, R.; Schlögl, R.; Dinse, K. P. *ChemCatChem* **2012**, *4*, 641−652.
(61) Baron, M.; Abbott, H.; Bondarchuk, O.; Stacchiola, D.; Uhl, A.; Shaikhutdinov, S.; Freund, H. J.; Popa, C.; Ganduglia-Pirovano, M. V.; Sauer, J. *Angew. Chem.* **2009**, *48*, 8006−8009.
(62) Klyushin, A. Y.; Rocha, T. C. R.; Haevecker, M.; Knop-Gericke, A.; Schloegl, R. *Phys. Chem. Chem. Phys.* **2014**, *16*, 7881−7886.
(63) Hävecker, M.; Cavalleri, M.; Herbert, R.; Follath, R.; Knop-Gericke, A.; Hess, C.; Hermann, K.; Schlögl, R. *Phys. Status Solidi B* **2009**, *246*, 1459−1469.
(64) Banares, M. A. *Catal. Today* **2005**, *100*, 71−77.
(65) Wachs, I. E. *Catal. Today* **2005**, *100*, 79−94.
(66) Reichenbächer, M.; Popp, J. *Challenges in Molecular Structure Determination*; Springer: Berlin, 2012.
(67) Yadav, L. D. S. *Organic Spectroscopy*; Kluwer Academic Publisher: New Delhi, 2005.
(68) Che, M.; Vedrine, J. *Characterization of Solid Materials and Heterogeneous Catalysts*; Wiley-VCH: Weinheim, 2012.
(69) Weil, J. A.; Bolton, J. R.; Wertz, J. E. *Electron Paramagnetic Resonance: Elementary Theory and Practical Applications*; Wiley: New York, 1994.
(70) Russell, A.; Stokes, J. *Ind. Eng. Chem.* **1946**, *38*, 1071−1074.
(71) Gao, X.; Bare, S.; Fierro, J. L.; Wachs, I. E. *J. Phys. Chem. B* **1999**, *103*, 618−629.
(72) Gao, X.; Bare, S.; Fierro, J. L.; Banarez, M. A.; Wachs, I. E. *J. Phys. Chem. B* **1998**, *102*, 5653−5666.
(73) Gao, X.; Bare, S.; Weckhuysen, B. M.; Wachs, I. E. *J. Phys. Chem. B* **1998**, *102*, 10842−10852.
(74) Banares, M. A.; Wachs, I. E. *J. Raman Spectrosc.* **2002**, *33*, 359−380.
(75) Vuurman, M. A.; Wachs, I. E. *J. Phys. Chem.* **1992**, *96*, 5008−5016.
(76) Gao, X.; Wachs, I. E. *J. Phys. Chem. B* **2000**, *104*, 1261−1268.
(77) Gao, X.; Jheng, J.; Wachs, I. E. *J. Catal.* **2002**, *209*, 43−50.
(78) Comité, A.; Sorrentino, A.; Capannelli, G.; Serio, M. D.; Tesser, R.; Santacesaria, E. *J. Mol. Catal., A* **2003**, *198*, 151−165.
(79) Monaci, R.; Rombi, E.; Solinas, V.; Sorrentino, A.; Santacesaria, E.; Colon, G. *Appl. Catal., A* **2001**, *214*, 203−212.
(80) Manganas, D.; Roemelt, M.; Hävecker, M.; Trunschke, A.; Knop-Gericke, A.; Schlögl, R.; Neese, F. *Phys. Chem. Chem. Phys.* **2013**, *15*, 7260−7276.
(81) Amakawa, K.; Sun, L.; Guo, C.; Hävecker, M.; Kube, P.; Wachs, I. E.; Lwin, S.; Frenkel, A. I.; Patlolla, A.; Hermann, K.; Schlögl, R.; Trunschke, A. *Angew. Chem., Int. Ed.* **2013**, *52*, 13553−13557.
(82) Jehng, J. M. *J. Phys. Chem. B* **1998**, *102*, 5816−5822.
(83) Gao, X.; Wachs, I. E. *J. Phys. Chem. B* **2000**, *104*, 1261−1268.
(84) Feng, Z.; Lu, J.; Feng, H.; Stair, P. C.; Elam, J. W.; Bedzyk, M. J. *J. Phys. Chem. Lett.* **2013**, *4*, 285−291. Feng, Z.; Cheng, L.; Kim, C. Y.; Elam, J. W.; Zhang, Z.; Curtiss, L. A.; Zapol, P.; Bedzyk, M. J. *J. Phys. Chem. Lett.* **2012**, *3*, 2845−2850. Banares, M. A.; Cardoso, J. H.; Agullo-Rueda, F.; Correa-Bueno, J. M.; Fierro, J. L. G. *Catal. Lett.* **2000**, *64*, 191−196.
(85) Rideal, E. *Proc. Cambridge Philos. Soc.* **1941**, *178*, 428.
(86) Eley, D.; Rideal, E. *Proc. R. Soc. London A* **1941**, *178*, 429−451.
(87) Langmuir, I. *Trans. Faraday. Soc.* **1921**, *17*, 621−654.
(88) Andersson, S. *Appl. Catal., A* **1994**, *112*, 209−218.
(89) Grabowski, R. *Appl. Catal., A* **2004**, *270*, 37−47.
(90) Creaser, D.; Andersson, B. *Appl. Catal., A* **1996**, *141*, 131−152.
(91) Chen, K.; Khodakov, A.; Yang, J.; Bell, A.; Iglesia, E. *J. Catal.* **1999**, *186*, 325−333.
(92) Routary, K.; Reddy, K.; Deo, G. *Appl. Catal., A* **2004**, *265*, 103−113.
(93) Vannice, A. *Catal. Today* **2007**, *123*, 18−22.
(94) Anderson, S. *Appl. Catal.* **1994**, *112*, 209−214.
(95) Grabowsky, R.; Sloczynski, J. *Chem. Eng. Process.* **2005**, *44*, 1082−1093.
(96) Grabowski, R.; Pietrzyk, S.; Słoczynski, J.; Genser, F.; Wcisło, K.; Grzybowska-Swierkosz, B. *Appl. Catal., A* **2002**, *232*, 277−288.
(97) Grabowski, R. *Appl. Catal., A* **2004**, *270*, 37−47.
(98) van Reijen, L. L.; Schuit, G. C. A. *Bull. Soc. Chim. Belg.* **1958**, *67*, 489−505.
(99) Schuit, G.; van Reijen, L. L. *Adv. Catal.* **1958**, *10*, 242−317.
(100) Creaser, D.; Anderson, B.; Hudgins, R.; Silverston, P. *J. Catal.* **1999**, *182*, 264−269.
(101) Cortez, G.; Fierro, J.; Banares, M. *Catal. Today* **2003**, *78*, 219−228.
(102) Karakoulia, S.; Triantafyllidis, K.; Tsilomenlekis, G.; Boghosian, S.; Lemonidou, A. *Catal. Today* **2009**, *141*, 245−253.
(103) Karakoulia, S. A.; Triantafyllidis, K. S.; Lemonidou, A. A. *Microporous Mesoporous Mater.* **2008**, *110*, 157−166.
(104) Gucbilmez, Y.; Dogu, T.; Balci, S. *Ind. Eng. Chem. Res.* **2006**, *45*, 3496−3502. Kondratenko, E. V.; Cherian, M.; Baerns, M.; Su, D.; Schlögl, R.; Wang, X.; Wachs, I. E. *J. Catal.* **2005**, *234*, 131−142.
(105) Schlögl, R. *Top. Catal.* **2011**, *54*, 627−638.
(106) Steinfeldt, N.; Müller, D.; Berndt, H. *Appl. Catal., A* **2004**, *272*, 201−213.
(107) Grabowski, R.; Sloczynski, J. *Chem. Eng. Process.* **2005**, *44*, 1082−1093.
(108) Grabowski, R. *Appl. Catal., A* **2004**, *270*, 37. Grabowski, R.; Grzybowska, B.; Samson, K.; Sloczynski, J.; Stoch, J.; Wcislo, K. *Appl. Catal., A* **1995**, *125*, 129−144.
(109) Teixeira-Neto, A. A.; Marchese, L.; Landi, G.; Lisi, L.; Pastore, H. O. *Catal. Today* **2008**, *133*−*135*, 1−6.
(110) Risini, C.; Panizza, M.; Arrighi, L.; Sechi, S.; Busca, G.; Miglio, R.; Rossini, S. *Chem. Eng. J.* **2002**, *89*, 75−87. Courcot, D.; Ponchel, A.; Grzybowska, B.; Barbaux, Y.; Rigole, M.; Guelton, M.; Bonnelle, J. P. *Catal. Today* **1997**, *33*, 109−118.
(111) Viparelli, P.; Ciambelli, P.; Lisi, L.; Ruoppolo, G.; Russo, G.; Volta, J. *Appl. Catal., A* **1999**, *184*, 291−301.
(112) Shee, D.; Rao, T.; Deo, G. *Catal. Today* **2006**, *118*, 288−297.
(113) Christodoulakis, A.; Machli, M.; Lemonidou, A.; Boghosian, S. *J. Catal.* **2004**, *222*, 293−306.
(114) Martra, G.; Arena, F.; Coluccia, S.; Frusteri, F.; Parmaliana, A. *Catal. Today* **2000**, *63*, 197−207.
(115) Lemonidou, A.; Nalbandian, L.; Vasalos, I. *Catal. Today* **2000**, *61*, 333−341.

(116) Heracleous, E.; Machli, M.; Lemonidou, A.; Vasalos, I. *J. Mol. Catal. A: Chem.* **2005**, *232*, 29−39.
(117) Arena, F.; Frusteri, F.; Parmaliana, A. *Catal. Lett.* **1999**, *60*, 59−63.
(118) Khodakov, A.; Olthof, B.; Bell, A. T.; Iglesia, E. *J. Catal.* **1999**, *181*, 205−216.
(119) Carrero, C. A.; Keturakis, C. J.; Orrego, A.; Schomäcker, R.; Wachs, I. E. *Dalton Trans.* **2013**, *42*, 12644−12653.
(120) Beck, B.; Harth, M.; Hamilton, N.; Carrero, C.; Uhlrich, J.; Trunschke, A.; Shaikhutdinov, S.; Schubert, H.; Freund, H. J.; Schloegl, R.; Sauer, J.; Schomaeker, R. *J. Catal.* **2012**, *296*, 120−131.
(121) Galinska, A.; Walendziewski, J. *Energy Fuels* **2005**, *19*, 1143−1147.
(122) Huang, B. S.; Chang, F. Y.; Wey, M. Y. *Int. J. Hydrogen Energy* **2010**, *35*, 7699−7705.
(123) Li, Y.; Xie, Y.; Peng, S.; Lu, G.; Li, S. *Chemosphere* **2006**, *63*, 1312−1318.
(124) Senevirathna, M. K. I; Pitigala, P. K. D. D. P.; Tennakone, K. *Sol. Energy Mater. Sol. Cells* **2006**, *90*, 2918−2923.
(125) Saleh, R. Y.; Wachs, I. E.; Chan, S. S.; Chersich, C. C. *J. Catal.* **1986**, *98*, 102−114.
(126) Pieck, C.; Banares, M. A.; Fierro, J. L. *J. Catal.* **2004**, *224*, 1−7.
(127) Chen, K.; Bell, A. T.; Iglesia, E. *J. Phys. Chem. B* **2000**, *104*, 1292−1299.
(128) Chen, K.; Bell, A. T.; Iglesia, E. *J. Catal.* **2002**, *209*, 35−42.
(129) Schwarz, O.; Habel, D.; Ovsitser, O.; Kondratenko, E.; Hess, C.; Schomäcker, R.; Schubert, H. *J. Mol. Catal. A: Chem.* **2008**, *293*, 45−52.
(130) Frank, B.; Dinse, A.; Ovsitser, O.; Kondratenko, E.; Schomäcker, R. *Appl. Catal., A* **2007**, *323*, 66−76.
(131) Kondratenko, E.; Baerns, M. *Appl. Catal., A* **2001**, *222*, 133−143.
(132) Argyle, M.; Chen, K.; Bell, A. T.; Iglesia, E. *J. Catal.* **2002**, *208*, 139−149.
(133) Cortez, G.; Fierro, J.; Banares, M. *Catal. Today* **2003**, *78*, 219−228.
(134) Bottino, A.; Capannelli, G.; Comite, A.; Storace, S.; Felice, R. D. *Chem. Eng. J.* **2003**, *94*, 11−18.
(135) Rao, T. V. M; Deo, G. *AIChE J.* **2007**, *53*, 1538−1549.
(136) Liu, Y. M.; Cao, Y.; Yan, S. R.; Dai, W. L.; Fan, K. N. *Catal. Lett.* **2003**, *88*, 61−67.
(137) Xu, J.; Chen, M.; Liu, Y.; Cao, Y.; He, H.; Fan, K. *Microporous Mesoporous Mater.* **2008**, *118*, 354−362.
(138) Dinse, A.; Khennache, S.; Frank, B.; Hess, C.; Herbert, R.; Wrabetz, S.; Schlögl, R.; Schomäcker, R. *J. Mol. Catal. A: Chem.* **2009**, *307*, 43−50.
(139) Puglisi, M.; Arena, F.; Frusteri, F.; Sokolovskii, V.; Parmaliana, A. *Catal. Lett.* **1996**, *41*, 41−43.
(140) Karakoulia, S.; Triantafyllidis, K.; Tsilomenlekis, G.; Boghosian, S.; Lemonidou, A. *Catal. Today* **2009**, *141*, 245−253.
(141) Gruene, P.; Wollfram, T.; Pelzer, K.; Schlögl, R.; Trunschke, A. *Catal. Today* **2010**, *157*, 137−142.
(142) Pena, M.; Dejoz, A.; Fornes, V.; Rey, F.; Vazquez, M.; Nieto, J. *Appl. Catal., A* **2001**, *209*, 155−164.
(143) Karakoulia, S. A.; Triantafyllidis, K. S.; Lemonidou, A. A. *Microporous Mesoporous Mater.* **2008**, *110*, 157−166.
(144) Solsona, B.; Blasco, T.; Nieto, J.; Pena, M.; Rey, F.; Vidal-Moya, A. *J. Catal.* **2001**, *203*, 443−452.
(145) Zhou, R.; Cao, Y.; Yan, S.; Deng, J.; Liao, Y.; Hong, B. *Catal. Lett.* **2001**, *75*, 107−112.
(146) Liu, Y.; Xie, S.; Cao, Y.; He, H.; Fan, K. *J. Phys. Chem. C* **2010**, *114*, 5941−5946.
(147) Watlin, T.; Deo, G.; Seshan, K.; Wachs, I. E.; Lercher, J. *Catal. Today* **1996**, *28*, 139−145.
(148) Deo, G.; Wachs, I. E. *J. Catal.* **1994**, *146*, 323−334.
(149) Martínez-Huerta, M. V.; Gao, X.; Tian, H.; Wachs, I. E.; Fierro, J. L.; Banares, M. A. *Catal. Today* **2006**, *118*, 279−287.
(150) Dunn, J. P.; Stenger, H. G., Jr; Wachs, I. E. *Catal. Today* **1999**, *51*, 301−318.
(151) Kondratenko, E.; Steinfeldt, N.; Baerns, M. *Phys. Chem. Chem. Phys.* **2006**, *8*, 1624−1633.
(152) Rossetti, I.; Mancinni, G.; Ghigna, P.; Scavani, M.; Piumetti, M.; Bonelli, B.; Cavani, F.; Comite, A. *J. Phys. Chem. C* **2012**, *116*, 22386−22389.
(153) Alexopoulos, K.; Reyniers, M. F.; Marin, G. *J. Catal.* **2012**, *289*, 127−139.
(154) Rozanska, X.; Fortrie, R.; Sauer, J. *J. Phys. Chem. C* **2007**, *111*, 6041−6050.
(155) (a) Nguyen, N. H.; Tran, T. H.; Nguyen, M. T.; Le, M. C. *Int. J. Quantum Chem.* **2010**, *110*, 2653−2670. (b) Zhao, C.; Wachs, I. E. *J. Catal. C* **2008**, *257*, 181−189.
(156) Cheng, M.; Chenoweth, K.; Oxgaard, J.; van Duin, A.; Goddard, W. A. *J. Phys. Chem. C* **2007**, *111*, 5115−5127.
(157) Chen, K.; Iglesia, E.; Bell, A. T. *J. Catal.* **2000**, *192*, 197−203.
(158) Chen, K.; Iglesia, E.; Bell, A. *J. Phys. Chem. B* **2001**, *105*, 646−653.
(159) Argyle, M.; Chen, K.; Iglesia, E.; Bell, A. T. *J. Phys. Chem. B* **2005**, *109*, 2414−2419.
(160) Rozanska, X.; Sauer, J. *J. Phys. Chem. A* **2009**, *113*, 11586−11594.
(161) Feyel, S.; Schöder, D.; Rozanska, X.; Sauer, J.; Schwarz, H. *Angew. Chem., Int. Ed.* **2006**, *45*, 4677−4681.
(162) Döbler, J.; Pritzsche, M.; Sauer, J. *J. Am. Chem. Soc.* **2005**, *127*, 10861−10868.
(163) Goodow, A.; Bell, A. T. *J. Phys. Chem. C* **2008**, *112*, 13204−13214.
(164) Rozanska, X.; Sauer, J. *Int. J. Quantum Chem.* **2008**, *108*, 2223−2229.
(165) Vining, W.; Goodow, A.; Bell, A. T. *J. Catal.* **2010**, *270*, 163−171.
(166) Gilardoni, F.; Bell, A. T.; Chakraborty, A.; Boulet, P. *J. Phys. Chem. B* **2000**, *104*, 12250−12255.
(167) Fu, H.; Liu, Z. P.; Li, Z. H.; Wang, W. N.; Fan, K. N. *J. Am. Chem. Soc.* **2006**, *128*, 11114−11123.
(168) Dai, G. L.; Li, Z. H.; Lu, J.; Wang, W. N.; Fan, K. N. *J. Phys. Chem. C* **2012**, *116*, 807−817.
(169) Gaertner, C. A.; Veen, A. C. V.; Lercher, J. A. *ChemCatChem* **2013**, *5*, 3196−3217.
(170) Sauer, J. In *Computational Modeling for Homogeneous and Enzymatic Catalysis*; Morokuma, K., Musaev, D. G., Eds.; Wiley-VCH: Weinheim, 2008; pp 231−244.
(171) Sauer, J.; Döbler, J. *Dalton Trans.* **2004**, *19*, 3116−3121.
(172) Schwarz, O.; Duong, P. Q.; Schaefer, G. *Chem. Eng. J.* **2009**, *145*, 420−428.
(173) Carrero, C.; Kauer, M.; Dinse, A.; Wolfram, T.; Hamilton, N.; Trunschke, A.; Schloegl, R.; Schomaecker, R. *Catal. Sci. Technol.* **2014**, *4*, 786−794.